Journal of Basic and Environmental Sciences, 8 (2021) 97-123

ISSN
Online:2356-6388
Print : 2536-9202

Research paper Open Access

Application of Aluminium ferrisilicate/ Salophene Schiff base composite for uranium (VI) adsorption from sulfate leach liquor

Lamia A. Yousef and Ahmad A. Ahmad
Nuclear Materials Authority, P.O.Box 530 El Maadi, Cairo, Egypt.
*Corresponding author's email: drlamiayousef_77@live.com

Abstract

Aluminium ferrisilicate (AFS) and / aluminium ferrisilicate Salophene Schiff base composites were prepared, characterized and tested for uranium (VI) adsorption from sulfate leach liquor using batch experiment technique. The effect of adsorption parameters such as pH value, composite dose, initial uranium concentration, shaking time, interfering ions and temperature were investigated and optimized. The kinetics of uranium adsorption by (AFS) and (AFS/ Salophene Schiff base) composites were studied using Lagergren pseudo-first order, pseudo-second order, Elovich, liquid film diffusion and intra-particle diffusion models. The pseudo-second order model was more suitable for our experiment. These data show that the process was exothermic and spontaneous. Testing of each composite for different adsorption isotherms revealed that the achieved experimental data were fitting well with the Langmuir and Dubinin–Radushkevich isotherm models. Using 0.25M H_2SO_4 acid solution, uranium (VI) ions was desorbed efficiently, and the composites were successfully regenerated. The optimum conditions were applied for adsorption and precipitation of uranium from cataclastic rocks, Abu Rusheid leach liquor, south Eastern De nsert, Egypt.

***Keywords*:** AFS, Salophene Schiff base, Adsorption, Uranium, Kinetics, Thermodynamics, Desorption.
Received; 30 April 2021, Revised form; 15 June 2021, Accepted; 15 June 2021, Available online 1 July 2021

1. Introduction

Uranium is a toxic heavy metal arising from the nuclear industry. The hexavalent uranyl ion is found to be the most stable and its compounds can cause potential carcinogens [1–3]. Thus, the effective recovery of uranium from acidic solution has been done such as chemical precipitation [4], membrane dialysis [5], solvent extraction [6], flotation [7], and adsorption [8–11]. Among these methods, adsorption appears to be one of the most effective methods due to its cost effective for removing the trace ions [12,13]. Different types of adsorbents have been developed and tested for recovery of uranium (VI) from aqueous media [14–17].

Many synthetic composites are used in adsorption of uranium, for instance, rice husk ash with aluminium oxide [18], composites based on active carbon [19-21], iron in haematite [22]. Activated carbon – aluminum ferrisilicate composite is used in adsorption of uranium [23]. Silicate mercapto Duolite composite (SMDC) and activated Duolite A 101 D (AD) were synthesized, characterized, and tested for uranium ions adsorption [24]. Manganese oxide coated zeolite modified with trioctyl amine (MOCZ/TOA) was tested for adsorption of uranium [25]. A zirconium molybdophosphate composite was designed for the selective recovery of uranium ions [26]. Uranium was adsorbed using bentonite treated with 1-amino 2-naphthol 4-sulfonic acid (ANSA) [27]. Dowex50WX8 modified with Alizarin Red S (ARS) was synthesised and its application on granitic samples, South Um Tawat, Eastern Desert [28]. Quinoline Silicate Lewatit Composite and activated Lewatit were prepared and tested for uranium removal from sulfate solution [29].

Among numerous adsorbents, most of the effective adsorbents are organic compounds combining nitrogen, oxygen, phosphorous and sulfur in their structures. Schiff bases, with RC=NR` as general formula, can form very stable complexes with transition metal ions which give rise to particularly potential adsorbents. The adsorptive actions of Schiff bases are usually attributed to their interactions of unshared electron pairs and π electrons with the metal ions through electrostatic attraction between the charged molecules and the charged metal. Schiff base ligands were applied for the removal of Cu^{2+}, Cd^{2+}, Co^{2+}, and Ni^{2+} from aqueous solutions [30]. Formaldehyde cross linked modified chitosan thioglyceraldehyde Schiff's base was used as adsorbents for the removal of Hg (II), Cu (II) and Zn

(II) from aqueous solutions [31]. A magnetic Schiff base (ferroferric oxide/ N,N-bis(3-methoxyl salicylic dene)-1,2-phenylenediamine) was removed uranium (VI) ions from aqueous solutions [32]. *O*-[1-(2-pyridylimino) ethyl] phenol (PEPh), was tested for uranium separation from carbonate leach liquor and determined by spectrophotometric determination technique [33]. In addition, other Schiff bases were used for uranium separation from aqueous solutions such as functionalized SBA-15 mesoporous silica with ethylenediamine-propylealicylaldimine [34], bis/salicylidene/ ethylenediamine [35], bis-salicylidene ethylene diamine with TOPO and TPPO [36], 2,2′-[1,2-phenylene bis(nitrilomethylidene)] bisphenol [37], N,N′-ethylenebis (4-propionyl-2,4-dihydro-5- methyl-2-phenyl-3H-pyrazol-3-oneimine) [38], tris-[2,4,6-(2-hydroxy-4-sulpho-1-naphthylazo)] -s-triazine [39], Calix [4] arene-based 8-hydroxy quinoline [40].

The purpose of this work is investigating the feasibility of adsorption of uranium (VI) by AFS and AFS/ Salophene Schiff base composites. It provides a rapid and effective way for removing the uranium from sulfate solution after the adsorption process. The uranium (VI) adsorption was analyzed as functions of the parameters of solution; pH value, composite dose, contact time and temperature. The adsorption kinetics, isotherms, thermodynamics, regeneration and reusability of the composites have also been investigated. The optimum conditions were applied for adsorption and precipitation of uranium from Abu Rusheid leach liquor, south Eastern Desert, Egypt.

2. Experimental

2-1- Preparation of standard stock solution

All the chemicals and reagents used in this work are of the analytical grade. A uranium stock standard solution assaying 1000 ppm (mg/L) was prepared by dissolving 1.537 g of UO_2SO_4 of BDH Chemicals Ltd. Poole, England. Uranium ion is analyzed in the aqueous solution by the oxidimetric titration method against ammonium metavanadate after its reduction [41].

2.2. Chemicals and reagents

Ferric chloride and sodium metasilicate were purchased from Adwic chemicals company in Egypt. Aluminium chloride was purchased from Sigma-Aldrich USA. N-phenyl anthranilic acid and Arsenazo III were obtained from Merch, Germany. NaOH, HCl, H_2SO_4 and HNO_3 analytical grade were obtained from POCH S.A., Poland. Ammonium vanadate, bromine, Urea, KBr and $FeSO_4.7H_2O$ were obtained from Scharlau Chemie. S.A., Spain.

2.3. Instrumentation

The absorbance of uranium, SiO_2, Al_2O_3, TiO_2, and P_2O_5 was measured using Metertech Inc, model SP-8001, UV-visible spectrophotometer. Na^+ and K^+ were determined by a Sherwood flame photometer model 410 (England). CaO, MgO and total iron content were determined volumetrically [42]. Trace elements and uranium of Abu Rusheid leach liquor were detected using ICP-OES [43].

The functional groups of aluminium ferrisilicate (AFS) and AFS/ Salophene Schiff base composites were characterized using FTIR (Thermo Scientific - NICOLET IS10 USA) spectrometer, before and after uranium adsorption. Scanning electron microscope (SEM) was used illustrate the surface morphology of (AFS) and (AFS/ Salophene Schiff base) composites before and after uranium adsorption. To identify the chemical composition of the (AFS) and (AFS/ Salophene Schiff base) composites before and after adsorption with uranium (VI) ions were subjected to Energy Dispersive X-Ray Analysis, (EDX). The composite of AFS/ Salophene Schiff base was identified at laboratories of the Atomic Energy Authority, Anshas, Egypt using CHNS analysis.

Two composites of (AFS) and (AFS/ Salophene Schiff base) after uranium adsorption were determined using Philips sequent ion X-ray fluorescence spectrometer-2400 at the Egyptian Atomic Energy Authority Laboratories. The sample was ground to very fine powders, and then mixed with polyvinyl methacrylate as a binder to facilitate the pressing process. The mixture was pressed in aluminum sample holder of 40 mm diameter by a pressing machine at 20 psi.

2.4. Preparation Abu Rusheid leach liquor

The studied technology is used to leach uranium (1580 mg/Kg) from Abu Rusheid area, south Eastern Desert, Egypt. The leaching factors were optimized (leaching time: 2 hours, 3M H_2SO_4, particle size: -200 mesh, ambient room temp. and solid to liquid phase ratio of 1:3) that it verifies best uranium leaching efficiency (95 %) with minimum dissolution of impurities. The final leach liquor was prepared containing approximately (500.33 mg/L, U). Appropriate volume of Abu Rusheid leach liquor has been stirred with suitable weights of (AFS) and (AFS/ Salophene Schiff base) via batch technique. The chemical composition of major oxides and its leach liquor has been determined by spectrophotometrically and trace elements by ICP-OES. All data are shown in (Tables 1, 2 and 3).

Table (1): Chemical composition of major oxide (wt %).

Oxide	SiO_2	Al_2O_3	$Fe_2O_3^T$	CaO	MgO	P_2O_5	Na_2O	K_2O	MnO	TiO_2	L.O.I
Wt,%	70.0	12.50	3.5	2.0	2.63	1.12	2.65	3.5	0.07	0.12	1.58

Table (2): Trace elements content (mg/kg) using ICP-OES technique.

Element	Ba	Mo	Zr	Pb	Cr	Cd	Co	Cu	Zn	V	U
Conc., mg/Kg	60	2.0	200	60	10.0	4.0	2.58	65	1800	2.0	1580

Table (3): Chemical composition of cataclastic rocks, Abu Rusheid leach liquor.

Ions	Si^{4+}	Al^{3+}	Fe^{3+}	Ca^{2+}	Mg^{2+}	P^{5+}	Na^{+}	K^{+}	Ti^{4+}	Mn^{2+}	
Conc., g/L	2.17	3.25	1.22	0.714	0.789	0.488	1.96	3.38	0.023	0.036	
Ions	Mo^{6+}	Ba^{2+}	Zr^{4+}	Cr^{3+}	Pb^{2+}	Cd^{3+}	Co^{2+}	Cu^{2+}	V^{5+}	Zn^{2+}	UO_2^{2+}
Conc., g/L	0.0005	0.016	0.053	0.0026	0.016	0.001	0.0006	0.017	0.0005	0.48	0.500

2.5. Synthesis of composites

2.5.1. Preparation of Aluminium ferrisilicate (AFS)

The composite was prepared by mixing 10 g of ferric chloride, 10 g of aluminium chloride, 40 g of sodium metasilicate and 30 g of sodium hydroxide in an agate mortar, and the mixture was polymerised at 750 °C for 2 hours. A powder was washed several times with distilled water till the filtrate pH reaches 7. The composite was dried at 120 °C, known as aluminium ferrisilicate (AFS) and shown in Scheme (A).

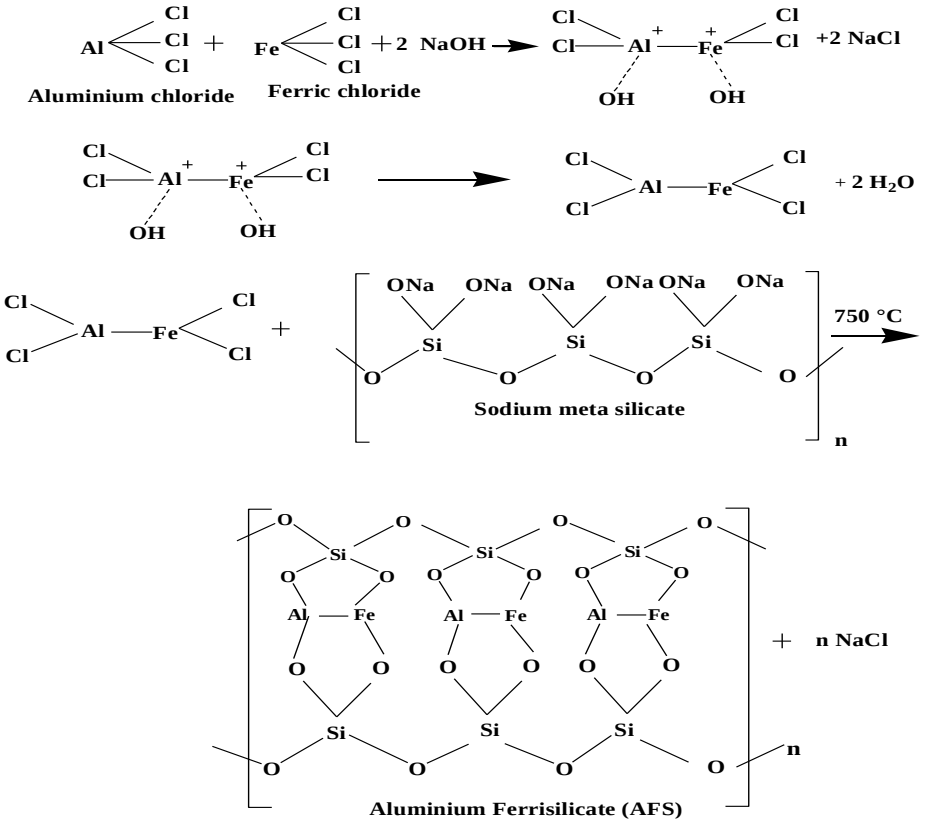

Scheme (A): Structure of Aluminium ferrisilicate (AFS)

2.5.2. Synthesis of Salophene Schiff base, [**N, N`-bis(3-methoxylsalicylidene)-1,2-phenylenediamine].**

A solution of o-phenylenediamine (1.08 g) dissolved in ethyl alcohol (10.0 mL) was added to a solution of o-Vanillin (3.04 g) in EtOH (10.0 mL). After being stirred at room temperature for 3 hours, the orange precipitate was obtained. The product of Salophene Schiff base was filtrated, washed twice with methanol and diethyl ether, then dried at 60 °C for 6 h, and obtained in Scheme (B).

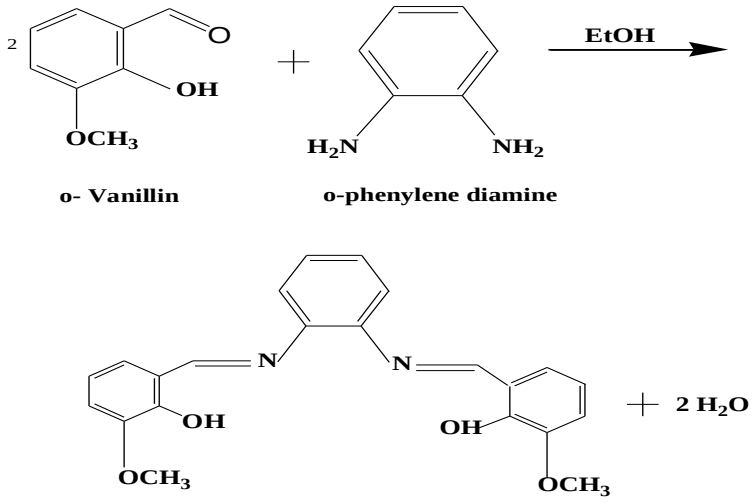

Scheme (B): Structure of Salophene, [N, N`-bis(3-methoxylsalicylidene)-1,2-phenylenediamine]

2.5.3. Preparation of Aluminium ferrisilicate/ Salophene Schiff base composite

A Salophene /sodium sulfate solution was prepared by dissolving 0.25 g Salophene and 0.25 g sodium sulfate in 100 mL distilled water. Afterward, 50 mL solution containing 1 g of (AFS) was added in the above system. Under stirring, the pH was adjusted to 2 for 2 hours. The (AFS/ Salophene Schiff base) was isolated and then dried in room temperature.

2.6. Adsorption Procedures

Factors optimization of U (VI) adsorption from synthetic solution by (AFS) and (AFS/ Salophene Schiff base) composites using batch technique; pH, contact time, initial uranium concentration, composite dose, temperature and interfering ions. In these experiments, 40 mL of synthetic uranium solution containing uranium concentrations were varied from 50 to 600 mg/L were mechanically shaken by stirring at 150 rpm with 0.1 g of each composite for a definite time ranging from 5 to 60 minutes at different temperatures. The uranium uptake capacity (q_e) in mg/g is calculated from the following equation:

$$q_e = (C_o - C_e) \times \frac{v}{m} \qquad \textbf{(1)}$$

Where C_o and C_e are the initial and equilibrium uranium concentrations (mg/L), respectively, and V, is volume of the aqueous solution (L) containing uranium and m, is the composite weight (g). In the mean time, the distribution coefficient (K_d) is calculated using the equation (2), where V, is the volume of the aqueous phase (mL):

$$K_d = \frac{C_o - C_e}{C_o} \times \frac{v}{m} \qquad \textbf{(2)}$$

2.7. Batch elution procedures

For uranium elution procedures, different eluting agents were studied to elute uranium from the loaded (AFS) and (AFS/ Salophene Schiff base**)** composites. Each experiment was performed by shaking 0.1 g of loaded composite with 40 mL of each individual eluting agent at different concentrations through a contact time of 30 min. at room temperature.

2.8. Analytical procedures

Uranium (VI) is analyzed in different aqueous phases by a single beam spectrophotometer, Meterch (SP-8001) using Arsenazo III indicator [44], at 650 nm wavelength against proper standard solution. The results were confirmed by the oxidometric titration method, Davies and Grey method, against ammonium meta-vanadate using N-phenyl anthranilic acid indicator [45].

3. Results and Discussion

3.1. Effect of initial uranium concentration

Studying the effect of uranium adsorption efficiency, as a function of initial uranium conc. is very important factor as we can determine the

maximum adsorption efficiency and uptake capacity for **(AFS)** and **(AFS/** Salophene Schiff base) composites. The plot of uranium adsorption against initial uranium concentration is presented in (Fig. 1) which shows two phases. In the first phase, uranium adsorption is constant from 50 to 150 mg/L because at low uranium concentration, number of uranyl ions is smaller than the number of active sites of the composite. In the second phase, the uranium adsorption is decreased from 150 to 600 mg/L due to the saturation of (AFS) active sites with uranyl ions. Accordingly, the maximum value of uranium uptake for (AFS) composite was 57 mg/g and optimum conc. at 150 mg/L U (VI). On the other hand, the maximum uptake for (AFS/ Salophene Schiff base) composite was 171 mg/g at conc. 450 mg/L U, (Fig.1).

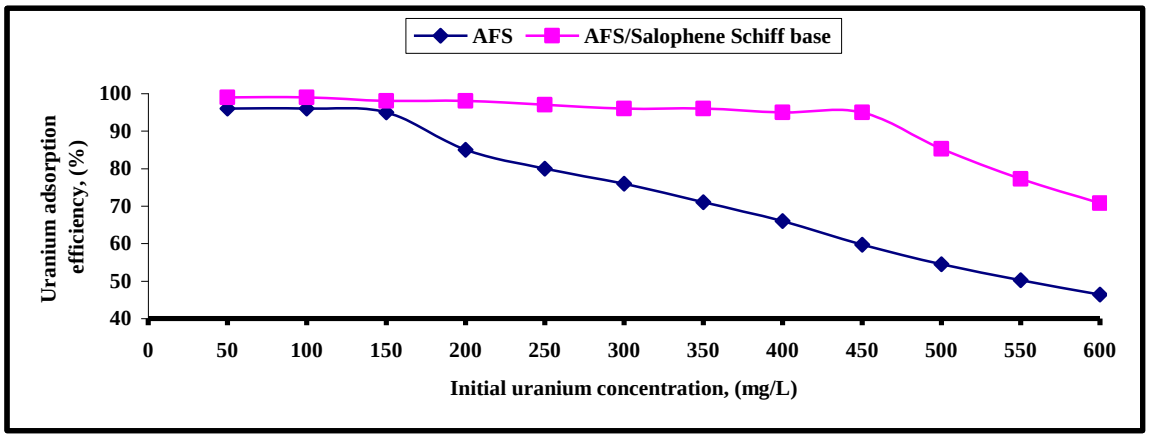

Fig. (1): Effect of initial uranium concentration on uranium adsorption efficiency by (AFS) and AFS/ Salophene Schiff base composites.
Adsorption conditions: pH: 2, composite dose: 0.1 g, volume: 40 mL, temperature: room temp., time: 30 min.

3.2. Effect of pH

The pH plays an important role in the retention of uranium to each composite, as pH can influence the aqueous chemistry of uranium and the properties of the active sites of the sorbent [46]. The effect of pH on the adsorption of uranium (VI) onto (AFS) and (AFS/ Salophene Schiff base) composites were carried out in the pH range of 1.0–6.0 using 40 mL uranium solution assaying 150 mg/L for (AFS) and 450 mg/L for (AFS/ Salophene Schiff base), 0.1 g dose, and 200 rpm stirring speed for 30 min. contact time at room temperature. The results obtained are shown in (Fig. 2) which indicates that uranium retention increases with increasing pH from 1 to 2 and reaches a maximum at pH 2, (q_e = 57 mg/g for AFS) and (qe= 171 mg/g for AFS/ Salophene Schiff base), then decreases with increasing pH from 2 to 6. The optimum pH for uranium retention on (AFS) and (AFS/ Salophene Schiff base) was pH 2.

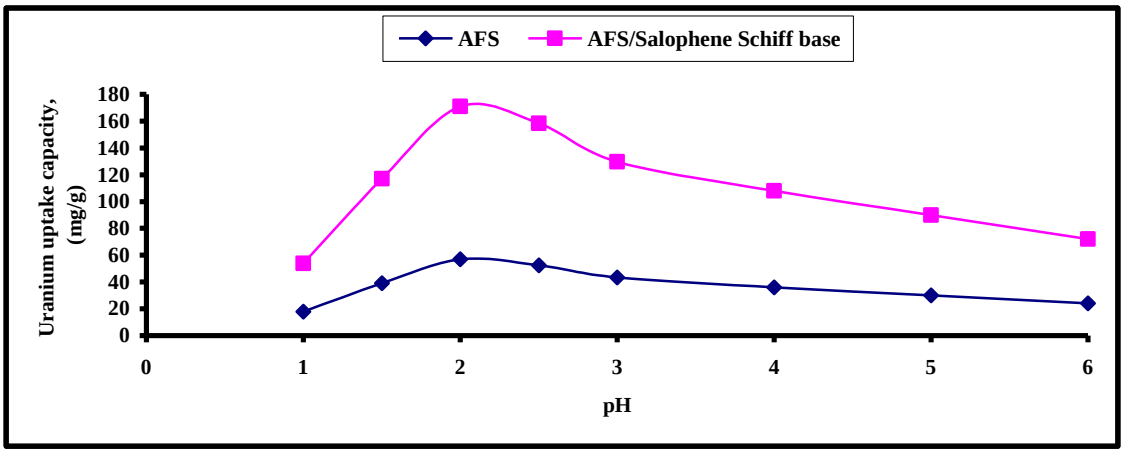

Fig. (2): Effect of pH on uranium uptake by (AFS) and AFS/ Salophene Schiff base composites.
Adsorption conditions: Uranium conc. 150 mg/L mixed with (AFS), Uranium conc. 450 mg/L mixed with (AFS/ Salophene Schiff base), composite dose: 0.1 g, volume: 40 mL, temperature: room temp., time: 30 min.

The possible coordination mechanism for the interaction between cationic species of uranium (UO_2^{2+}) and the Aluminum ferrisilicate (AFS) is shown in Scheme (C).

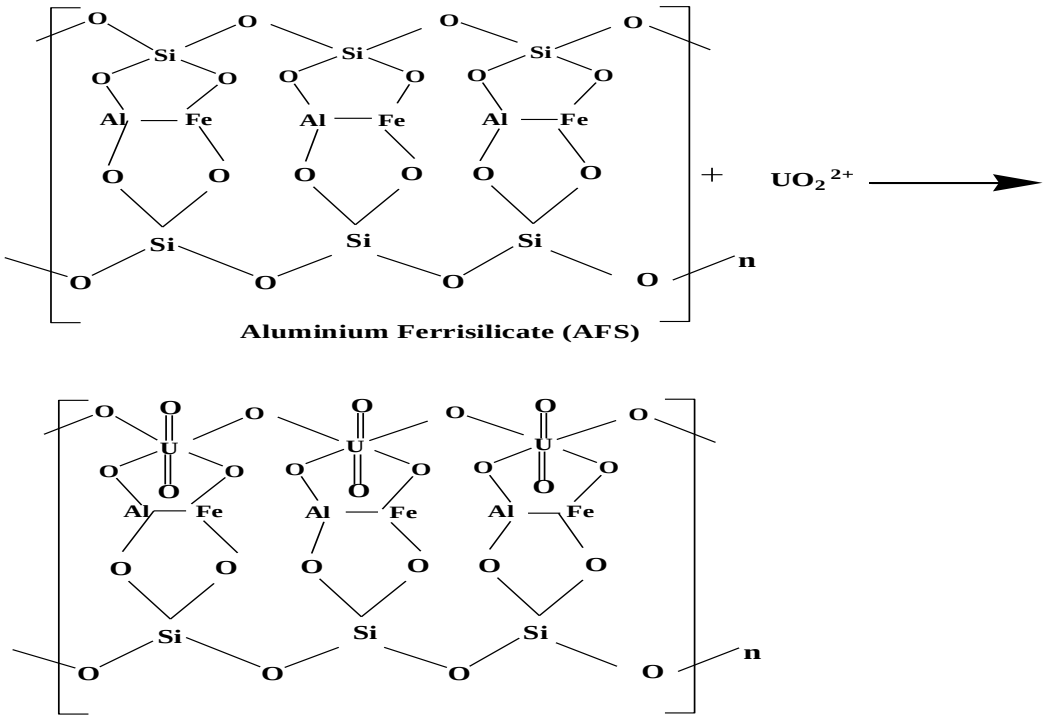

Scheme (C): Interaction between cationic species of (UO_2^{2+}) and AFS

The possible coordination mechanism for the interaction between cationic species of uranium UO_2^{2+} and the (AFS/ Salophene Schiff base) composite is shown in Scheme (D).

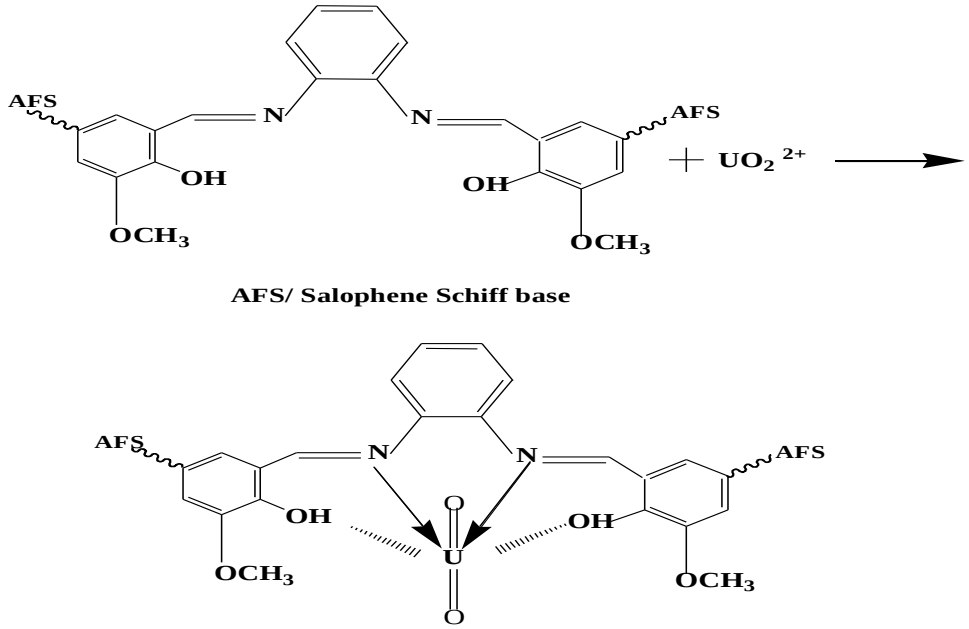

Scheme (D): Interaction between cationic species of (UO_2^{2+}) and the (AFS/ Salophene Schiff base) composite

The possible coordination mechanism for the interaction between anionic species of uranium (VI) sulfate; ($UO_2(SO_4)_2^{2-}$) and the AFS/ Salophene Schiff base composite is shown in Scheme (E).

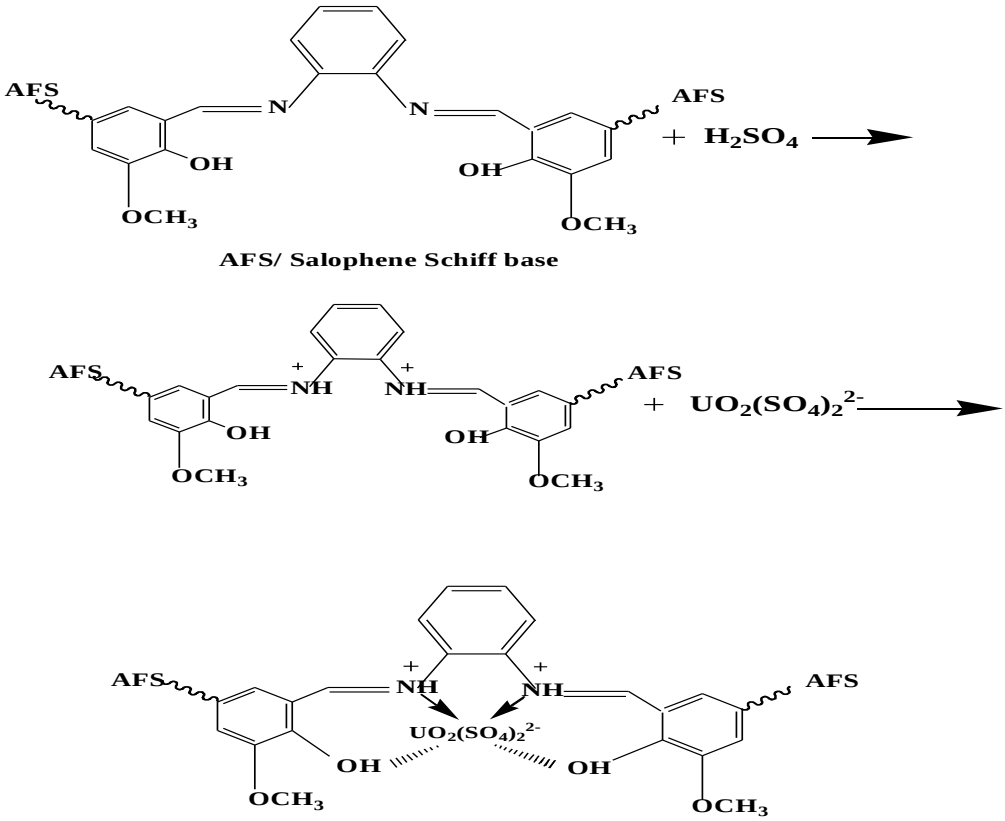

Scheme (E): Interaction between anionic species of ($UO_2(SO_4)_2^{2-}$) and AFS/ Salophene Schiff base composite

While the reaction between anionic species of uranium (VI) sulfate; ($UO_2(SO_4)_3^{4-}$) and AFS/ Salophene Schiff base composite is obtained in Scheme (F).

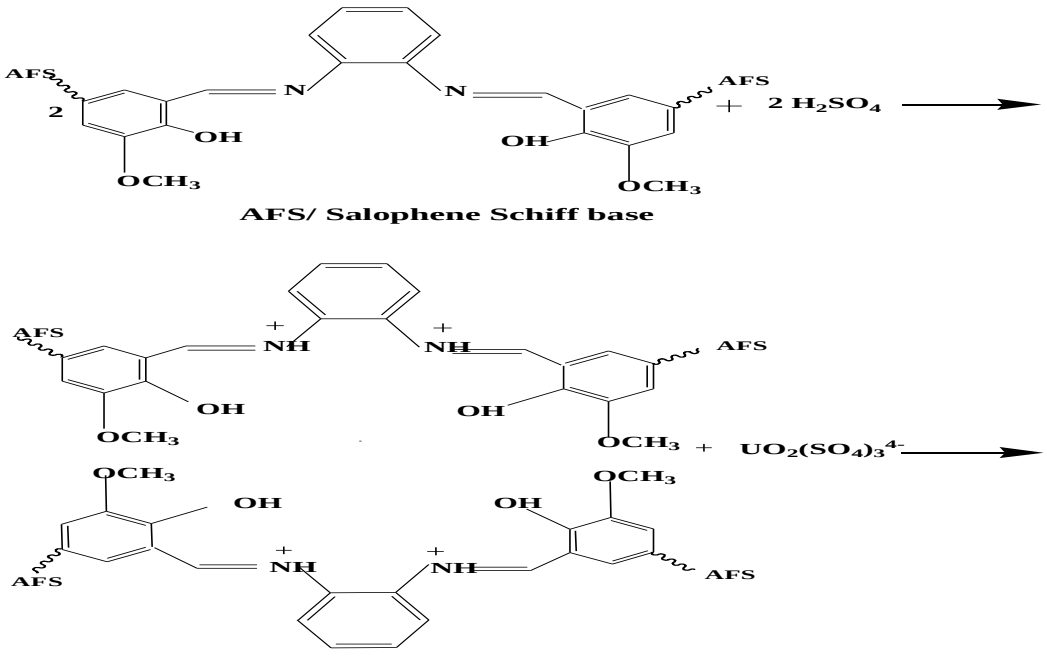

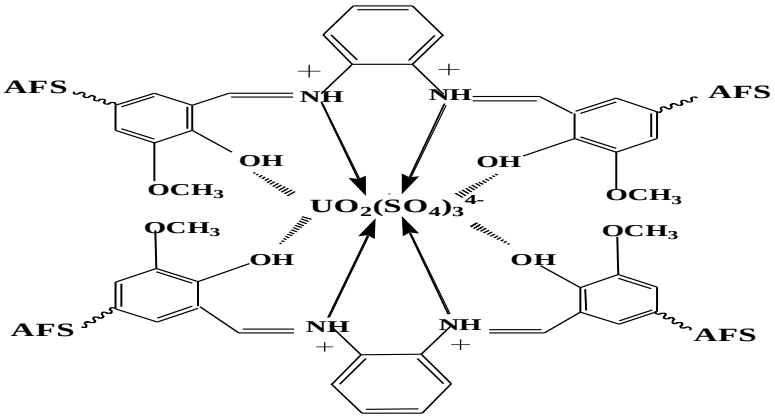

Scheme (F): Interaction between anionic species of $(UO_2(SO_4)_3^{4-})$ and AFS/ Salophene Schiff base composite

3.3. Effect of equilibrium time

The effect of equilibrium time as a function of uranium retention was investigated over time intervals from 5 to 60 min. through 0.1 g of (AFS) and (AFS/ Salophene Schiff base) mixing with 40 mL of uranium solution at pH 2. From the obtained results in (Fig. 3), the uranium uptake increases with increasing equilibrium time and reaches a maximum value (57 mg/g for AFS) and (171 mg/g for AFS/ Salophene Schiff base) at 30 min., thereafter, remaining almost constant up to 60 min. Therefore, 30 min. was sufficient to establish equilibrium and used in all subsequent studies.

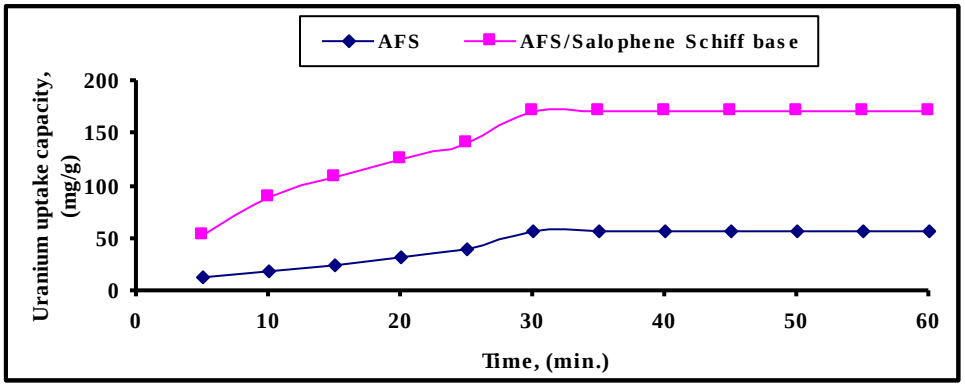

Fig. (3): Effect of time contact on uranium uptake by (AFS) and AFS/ Salophene Schiff base composites. Adsorption conditions: Uranium conc. 150 mg/L mixed with (AFS), Uranium conc. 450 mg/L mixed with (AFS/ Salophene Schiff base), composite dose: 0.1 g, volume: 40 mL, temperature: room temp., and pH 2.

3.3.1. Adsorption kinetic modeling

The kinetic modeling describes the rate of uranyl ions uptake onto (AFS) or (AFS/ Salophene Schiff base). The kinetic parameters are helpful for the prediction of adsorption rate and give important information for designing and modeling extraction processes. The mechanism of uranium adsorption by (AFS) or (AFS/ Salophene Schiff base) and the rate constants of the adsorption process were determined using pseudo-first order, pseudo-second order, Elovich model, Intra-particle diffusion and Liquid film diffusion were tested. The pseudo-first order kinetic model is represented by the following equation [47, 48]:

$$Log\,(q_e - q_t) = Log q_e - (\frac{K_1}{2.303})t \qquad (3)$$

Where K_1 (min.$^{-1}$) is the rate constant, qe the amount of metal adsorbed per unit mass at equilibrium and q_t is the amount adsorbed per unit time (t, min.$^{-1}$). Plotting Log (q_e-q_t) against t gives a straight line as shown in (Fig. 4), providing the first order adsorption rate constant K_1 and q_e values from its slope and intercept, respectively.

The plot diagram suggested the applicability of the pseudo-first order kinetic model to fit the practical data as given in (Table 4). The calculated value of q_e was found to attain (128.8 mg/g for AFS), and (344.11 mg/g for AFS/ Salophene Schiff base) which is not closest to the determined practical uptake capacity of (57 mg/g for AFS) and (171 mg/g for AFS/ Salophene Schiff base). The data obtained showed that the first order kinetic model is in not agreement with the experimental data and therefore is not suitable for explaining the studied system.

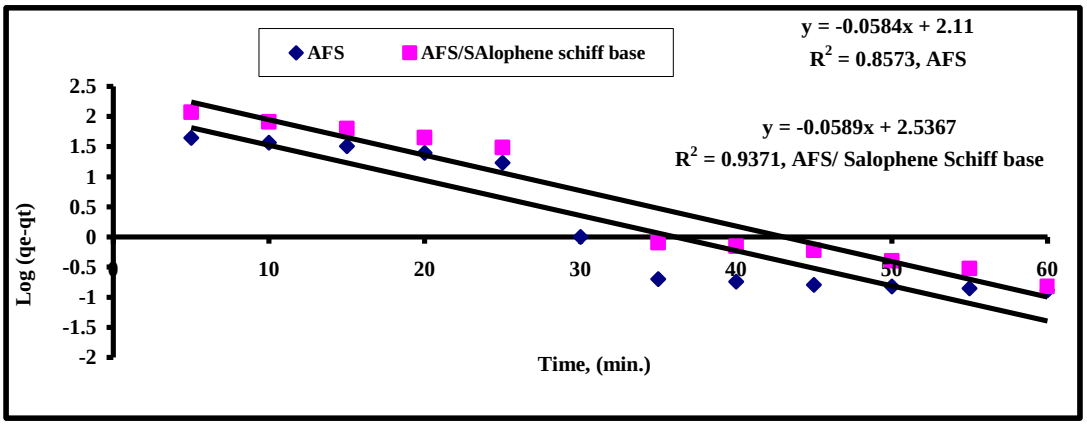

Fig. (4): Pseudo-first order model of uranium adsorption onto (AFS) and AFS/ Salophene Schiff base composites. Adsorption conditions: Uranium conc. 150 mg/L mixed with (AFS), Uranium conc. 450 mg/L mixed with (AFS/ Salophene Schiff base), composite dose: 0.1 g, volume: 40 mL, temperature: room temp., and pH 2.

On the other hand, the pseudo-second order kinetic model is represented by the following equation [49]:

$$\frac{t}{q_t} = \frac{1}{k_2 q_e^{\ 2}} + (\frac{1}{q_e})t \qquad (4)$$

Where K_2 is the rate constant (g/mg.min.). The straight line of plot t/q_t against t gives the slope $1/q_e$ and the intercept $1/k_2q^2_e$. Figure (5) suggested applicability of pseudo-second order kinetic model to fit the practical data as shown in (Table 4). The calculated value of q_e was found to be 58.82 for (AFS), and 172.41 for (AFS/ Salophene Schiff base).

The data showed that the second order kinetic model is in agreement with the experimental data 57 mg/g for (AFS) and 171 mg/g for (AFS/ Salophene Schiff base) and therefore is suitable for the studied adsorption system.

Table (4): Kinetic parameters of uranium adsorption onto (AFS) and (AFS/ Salophene Schiff base) composites.

Parameters	AFS	AFS/ Salophene Schiff base
	Pseudo-first order	
q_e, (mg/g) calculated	128.8	344.11
qe (mg/g) exp.	57	171
K_1	0.134	0.135
R^2	0.8573	0.9371
	Pseudo-second order	
q_e, (mg/g) calculated	58.82	172.41
qe (mg/g) exp.	57	171
K_2	0.00084	0.00054
R^2	0.9901	0.9914
	Elovich kinetic	
β, (g/mg)	0.046	0.0165
α, (mg/g min)	6.18	27.23
R^2	0.8203	0.9598
	Intra-particle Diffusion	
K, (mg g^{-1} $min^{-1/2}$)	12.274	33.329
C, (mg g^{-1})	-18.275	-19.39
qe (mg/g) exp.	57	171
R^2	0.8925	0.9826
	Liquid Film Diffusion	
K_f	0.0459	0.654
Intercept	0.0278	-0.0551
R^2	0.9587	0.9957

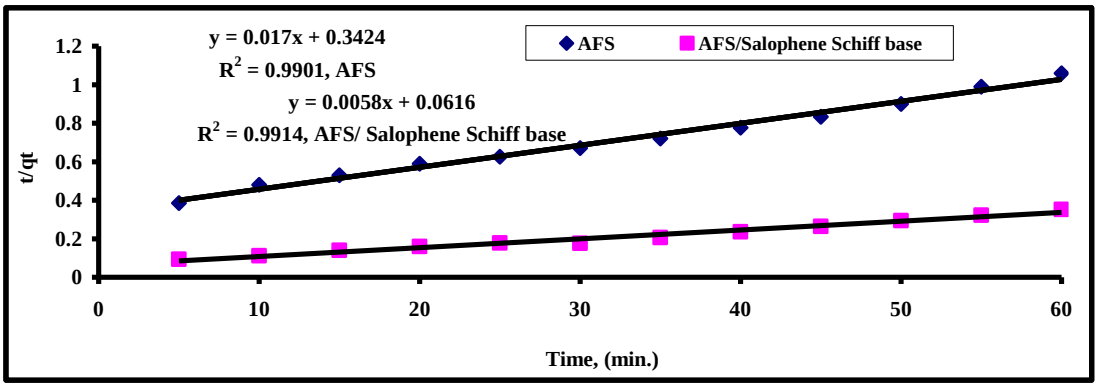

Fig. (5): Pseudo-second order model of uranium adsorption onto (AFS) and AFS/ Salophene Schiff base composites. Adsorption conditions: Uranium conc. 150 mg/L mixed with (AFS), Uranium conc. 450 mg/L mixed with (AFS/ Salophene Schiff base), composite dose: 0.1 g, volume: 40 mL, temperature: room temp., and pH 2.

The description of the adsorption mechanism for uranium (VI) onto (AFS) and (AFS/ Salophene Schiff base) composites could occur via the intra-particle diffusion model and the liquid film diffusion model; these explain the mechanism in steps: movement of uranium from the bulk of the solution to the (AFS) and (AFS/ Salophene Schiff base) surface (bulk diffusion) followed by uranium diffuse to (AFS) and (AFS/ Salophene Schiff base) surface from the boundary layer (film diffusion), then uranium transportation from surface to inner pores (intra-particle diffusion or pore diffusion); and finally the adsorption of uranium at active sites on the surface of the composites (ion exchange or chelation), [50- 52]. The intra-particle diffusion is presented by the following equation:

$$qt = k_i t^{0.5} + C \qquad (5)$$

where q_t is the adsorption capacity of uranium per unit mass of (AFS) and (AFS/ Salophene Schiff base) at time t. k_i is the intra-particle diffusion rate constant (mg g^{-1} $min^{-1/2}$), t is the time (min), and C is the intercept (mg g^{-1}); it donates the conception on the thickness of the boundary layer. We plot q_t against $t^{0.5}$. If the uranium adsorption onto (AFS) and (AFS/ Salophene Schiff base) fit with the intra-particle diffusion model as a controlling step, it produces a linear relationship, and the line passes to the origin [53].

The deviation of straight lines from the origin may be due to the difference in rate of mass transfer in the initial and final stages of adsorption. The first stage may be back to the uranium ions adsorption on the surface with macro-pore structure and so it is the fastest adsorption stage. The final stage may be regarded to the intra-particle diffusion through the mesopores and/or micropores while the last stage is equilibrium.

Figure (6) shows that the straight line did not pass through the origin; this implies that the intra-particle diffusion model was not the only controlling step; furthermore, this was a significance of some degree of boundary layer control. The values of intra-particle diffusion parameters are calculated in (Table 4). It is clear that the rate of adsorption not controlled only with the intra-particle diffusion model, but there are other process done.

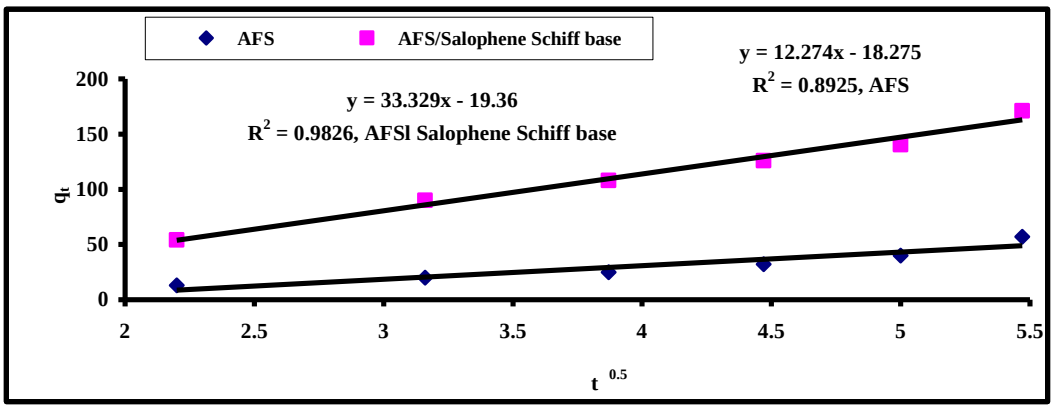

Fig. (6): The intra-particle diffusion model for uranium adsorption onto (AFS) and (AFS/ Salophene Schiff base) composites.
Adsorption conditions: Uranium conc. 150 mg/L mixed with (AFS), Uranium conc. 450 mg/L mixed with (AFS/ Salophene Schiff base), composite dose: 0.1 g, volume: 40 mL, temperature: room temp., and pH 2.

The liquid film diffusion model assumes that the flow of the adsorbate molecules through a liquid film surrounding the solid adsorbent is the slowest step in the adsorption process (i.e., the one that determines the kinetics of the rate processes). The liquid film diffusion model [54, 55] mathematically expressed in the equation:

$$Ln(1-F) = -K_f\, t \qquad (6)$$

where F was the fractional attainment of the equilibrium F= q_t /q_e. The parameter of K_f (min^{-1}) was the diffusion rate in the film diffusion model and t was the time per minute. A linear plot of Ln (1-F) vs. time, with a zero intercept, suggests that the kinetic of the adsorption process is controlled by diffusion through the liquid film around the (AFS) and (AFS/ Salophene Schiff base) composites. Figure (7) shows the straight-line relationship for time vs. Ln (1-F), it did not pass through the origin and liquid film diffusion model was not the controlling step. The values of K_f and intercept were calculated in Table (4). Accordingly, it can be concluded that the adsorption mechanism of uranium by (AFS) and (AFS/ Salophene Schiff base) composites was not controlled by the liquid film diffusion and the intra-particle diffusion.

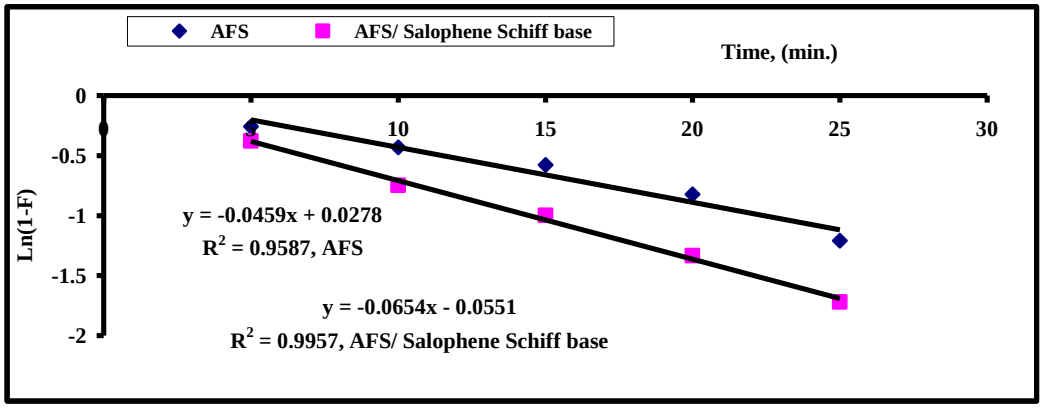

Fig. (7): The liquid film diffusion model for uranium adsorption onto (AFS) and (AFS/ Salophene Schiff base) composites.
Adsorption conditions: Uranium conc. 150 mg/L mixed with (AFS), Uranium conc. 450 mg/L mixed with (AFS/ Salophene Schiff base), composite dose: 0.1 g, volume: 40 mL, temperature: room temp., and pH 2.

The Elovich equation is another kinetic model frequently used to describe the adsorption of adsorbates such as uranium by solid adsorbent (AFS) ans AFS/ Salophene Schiff base composites from an aqueous medium. The linear form of the Elovich equation [56] could be written by the following equation:

$$qt = \frac{1}{\beta} Ln(\alpha\beta) + \frac{1}{\beta} Ln(t) \qquad (7)$$

where α and β are the Elovich coefficients. The parameter α is initial adsorption rate (mg/g min), and β is desorption constant related to extent of surface coverage and activation energy for chemisorptions (g/mg), respectively. The Elovich coefficients α and β are calculated from slope and intercept of the q_t vs. *Ln t*. plots shown in (Fig. 8) and their values are tabulated in Table (4). From (Fig. 8), it can be noted that the linear fit curves did not exhibit better adaptability with the Elovich model (R^2=0.8203 for AFS, and R^2=0.9598 for AFS/ Salophene Schiff base), demonstrating that the adsorption of uranium ions onto composites cannot be described using the Elovich model.

Comparing the correlation coefficients of five kinetic models, it clearly revealed that the pseudo-second-order model can be described the adsorption kinetic of uranium onto (AFS) and (AFS/ Salophene Schiff base) composites.

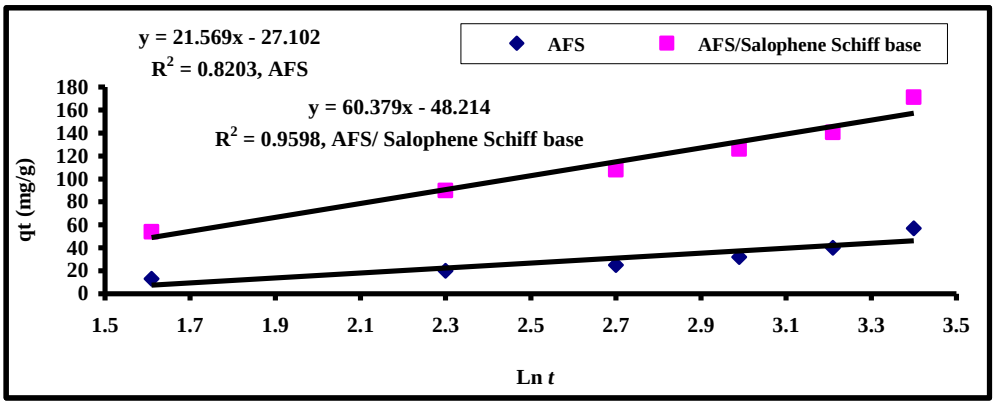

Fig. (8): Elovich kinetic model plots for the adsorption of uranium adsorption onto (AFS) and (AFS/ Salophene Schiff base) composites.
Adsorption conditions: Uranium conc. 150 mg/L mixed with (AFS), Uranium conc. 450 mg/L mixed with (AFS/ Salophene Schiff base), composite dose: 0.1 g, volume: 40 mL, temperature: room temp., and pH 2.

3.3.2. Adsorption isotherm modeling

The adsorbed amount of uranium on (AFS) and (AFS/ Salophene Schiff base) were determined as a function of uranyl ions concentration at equilibrium and ambient temperature. The Langmuir treatment [57] is based on the assumption that (a) maximum adsorption is corresponded to saturated monolayer of adsorbate molecules on the adsorbent surface, (b) the energy of adsorption is constant, (c) there is no trans-migration of adsorbate on the plane of the surface. The Langmuir isotherm model is represented by the following equation:

$$\frac{C_e}{q_e} = \frac{1}{q_e b} + \frac{C_e}{q_e} \qquad (8)$$

Where C_e is the concentration of uranium in the solution at equilibrium (mg/L), q_e is the amount of uranium adsorbed per weight unit of the adsorbent at equilibrium (mg/g), b are Langmuir constants related to maximum uptake capacity (mg/g) and adsorption energy (L/mg). The linear plot of C_e/q_e versus C_e shows that the adsorption process obeys Langmuir model as shown in (Fig. 9) and (Table 5).

The correlation coefficient for the linear regression fits of the Langmuir plot and found to be (R^2= 0.9982 for AFS) and (R^2= 0.9991 for AFS/ Salophene Schiff base). q_o and b were determined from the slope and intercept and were found to be (62.51 mg/g and 0.128 g/mg for AFS) and (175.43 mg/g and 0.240 g/mg for AFS/ Salophene Schiff base) respectively. The essential characteristics of Langmuir isotherm can be expressed in term of dimensionless constant, separation factor or equilibrium parameter, R_L, which is defined by the equation:

$$R_L = \frac{1}{1+bC_e} \qquad (9)$$

Where b is the Langmuir constant and C_o is the initial uranium (VI) conc., the values of R_L are in between 0 and 1 indicating favorable adsorption of uranium onto (AFS) and (AFS/ Salophene Schiff base), (Table 6).

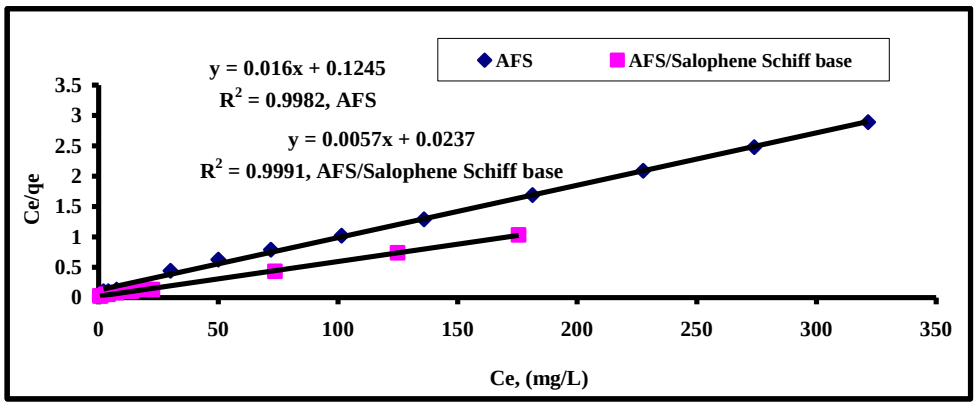

Fig. (9): Langmuir isotherm model of uranium adsorption onto (AFS) and AFS/ Salophene Schiff base composites.
Adsorption conditions: pH: 2, composite dose: 0.1 g, volume: 40 mL, temperature: room temp., time: 30 min.

Table (5): Adsorption isotherm of uranium adsorption onto (AFS) and AFS/ Salophene Schiff base composites.

Parameters	AFS	AFS/ Salophene Schiff base
	Langmuir isotherm	
q_e, (mg/g) calculated	62.51	175.43
qe (mg/g) exp.	57	171
b (g/mg)	0.128	0.240
R^2	0.9982	0.9991
	Freundlich isotherm	
q_e, (mg/g) calculated	23.23	41.26
qe (mg/g) exp.	57	171
n	3.36	2.86
R^2	0.8996	0.8479
	Temkin isotherm	
B, (J mol^{-1})	3.7295	29.032
b	664.317	85.33
A, (Lg^{-1})	7830.7	4.539
R^2	0.4453	0.9066
	Dubinin–Radushkevich isotherm	
q_m , (mg/g) calculated	58.98	174.98
q_e, (mg/g) exp.	57	171
Slope	$-1* 10^{-6}$	$-3* 10^{-7}$
β , (mol^2/kJ^2)	$1* 10^{-9}$	$3* 10^{-10}$
E, (kJ/mol)	22.36	40.82
R^2	0.9918	0.9942
	Jovanovic isotherm	
q_{max}, (mg/g) calculated	14.79	39.56
qe (mg/g) exp.	57	171
K_j, (Jovanovic constant)	-0.1887	-0.0751
R^2	0.9078	0.7586

Table (6): Calculated values of the equilibrium parameter, R_L of Langmuir model for each composites (AFS) and (AFS/ Salophene Schiff base).

Uranium conc., (mg/L)	50	100	150	200	250	300	350	400	450	500	550	600
R_L, (AFS)	0.135	0.072	0.049	0.037	0.030	0.025	0.021	0.019	0.017	0.015	0.014	0.012
R_L, (AFS/ Salophene Schiff base)	0.076	0.04	0.027	0.020	0.016	0.013	0.011	0.010	0.0091	0.0082	0.0075	0.0068

The Freundlich isotherm model [58] was also applied to the adsorption. This equation is basically empirical but is often useful as a means of data description. The Freundlich isotherm model is represented by the equation:

$$Logq_e = LogK_f + (\frac{1}{n}).LogC_e \qquad (10)$$

Where C_e is the equilibrium conc., (mg/L) and q_e the amount of uranium ions adsorbed at equilibrium, while K_f and n are the Freundlich constants standing for uptake capacity (mg/g) and adsorption intensity respectively. A plot of Log q_e versus Log C_e, (Fig. 10), is linear and the constants K_f and n were found to be (23.23 mg/g and 3.36 for AFS), and (41.26 mg/g and 2.86 for AFS/ Salophene Schiff base), respectively. The correlation coefficient (R^2) of Freundlich plot was found to be (R^2= 0.8996 for AFS) and (R^2= 0.8479 for AFS/ Salophene Schiff base) indicating that the experiments data of Langmuir are better than Freundlich (Table 5).

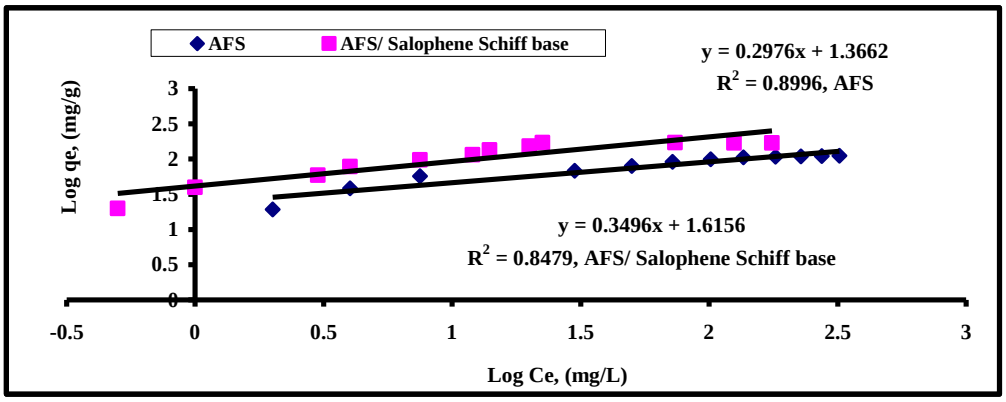

Fig. (10): Freundlich isotherm model of uranium (VI) adsorption onto (AFS) and AFS/ Salophene Schiff base composites.
Adsorption conditions: pH: 2, composite dose: 0.1 g, volume: 40 mL, temperature: room temp., time: 30 min.

Temkin isotherm model takes the effects of adsorbate/ adsorbate interactions on the adsorption process; it is also assumed that the heat of adsorption (ΔH ads) of all molecules in the layer decreases linearly as a result of increase surface coverage [59, 60]. The linear form of Temkin isotherm model is given by the following [61, 62]:

$$q_e = \frac{RT}{b} LnA + \frac{RT}{b} LnC_e \qquad (11)$$

$$B = \frac{RT}{b} \qquad (12)$$

where b is Temkin isotherm constant, A is Temkin isotherm constant (L g^{-1}), R is universal gas constant (8.314 J/mol. ˚K), T is temperature at 298 ˚K and B is Temkin constant related to heat of sorption (J mol^{-1}). The parameters of q_e (mg g^{-1}) and C_e (mg L^{-1}) are the equilibrium concentrations of U (VI) in the solid and liquid phase, respectively. Plotting q_e versus Ln C_e should give a straight line if the adsorption energy decreases linearly with increasing surface coverage, (Fig. 11). All Temkin parameters are shown in (Table 5). According to the given relation of q_e versus Ln C_e, the value of (A) constant for (AFS) and AFS/ Salophene Schiff base composites were 7830.7 and 4.539 (L g^{-1}) , while the value of (B) constant for each composite were 3.7295 and 29.032 (J mol^{-1}) respectively. The correlation coefficient (R^2) of Temkin isotherm for (AFS) and AFS/ Salophene Schiff base were observed 0.4453 and 0.9066 respectively, which are lower than (R^2) of Langmuir isotherm. Temkin isotherm did not fit to describe the adsorption isotherm.

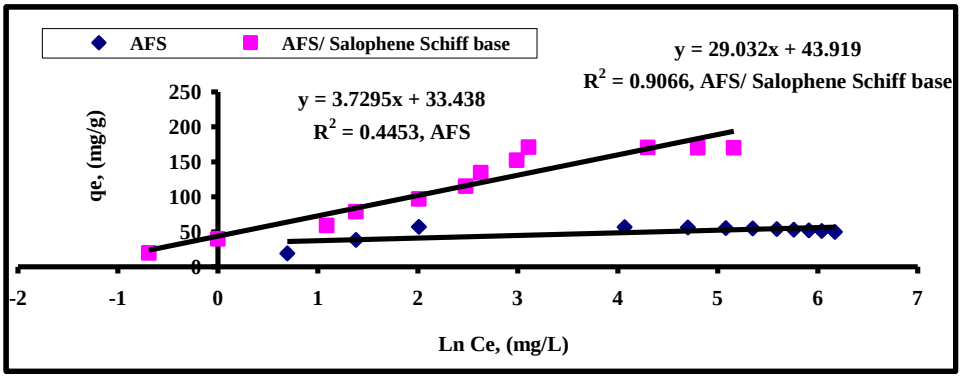

Fig. (11): Temkin isotherm for uranium adsorption onto (AFS) and (AFS/ Salophene Schiff base) composites.
Adsorption conditions: pH: 2, composite dose: 0.1 g, volume: 40 mL, temperature: room temp., time: 30 min.

The Dubinin–Radushkevich isotherm model is used to denote the adsorption mechanism with energy distribution. The model has a temperature-dependent used to estimate the characteristic porosity in addition to the apparent energy of adsorption. The Dubinin–Radushkevich isotherm equation is linearly represented as follows:

$$Lnq_e = Lnq_m - \beta\varepsilon^2 \qquad (13)$$

$$\varepsilon = RT\,.Ln\left(1+\frac{1}{C_e}\right) \qquad (14)$$

where q_e (mg/g) is the adsorbed value of the uranyl ion at equilibrium concentration, q_m is the theoretical

isotherm saturation capacity (mg/g), β is the Dubinin- Radushkevich isotherm constant (mol^2 /kJ^2), ε is the polanyl potential, C_e (mg/L) is U(VI) concentration in leach liquor at equilibrium, R is the gas constant (8.314 J/mol ˚K) and T (˚K) is the absolute temperature. The mean adsorption energy E (J/mol) of adsorption of uranyl ions onto the (AFS) and AFS / Salophene Schiff base composites can be estimated from the following equation:

$$E = \frac{1}{\sqrt{2\beta}} \qquad (15)$$

If the adsorption energy is (8 - 16 kJ/mol), the sorption process is supposed to proceed via chemisorption, but if E is less than 8 kJ/mol, the sorption process is physisorption [63, 64]. A plot of Ln q_e versus the square of potential energy ε^2 where q_m and β are calculated from the slope and intercept of the linear plots (Fig. 12) and all parameters are shown in Table (5). The mean adsorption energy (E) of adsorption of uranyl ions onto (AFS) and AFS / Salophene Schiff base composites is calculated to be 22.36 and 40.82 kJ/mol which are actually within the energy range of chemical sorption (E > 8 kJ/mol). This indicates that the sorption of uranium onto (AFS) and AFS / Salophene Schiff base composites is chemical in nature.

Testing of each composite for Dubinin-Radushkevich adsorption isotherm revealed that the achieved experimental data were fitting well with the Dubinin–Radushkevich isotherm model with 58.98 mg/g as theoretical capacity for (AFS) composite; while 174.98 mg/g as for (AFS/ Salophene Schiff base) composite, respectively. This indicates that the adsorption of uranium onto two composites is best described by Dubinin–Radushkevich isotherm model which contributed to the adsorption by chemical complexation / ion exchange.

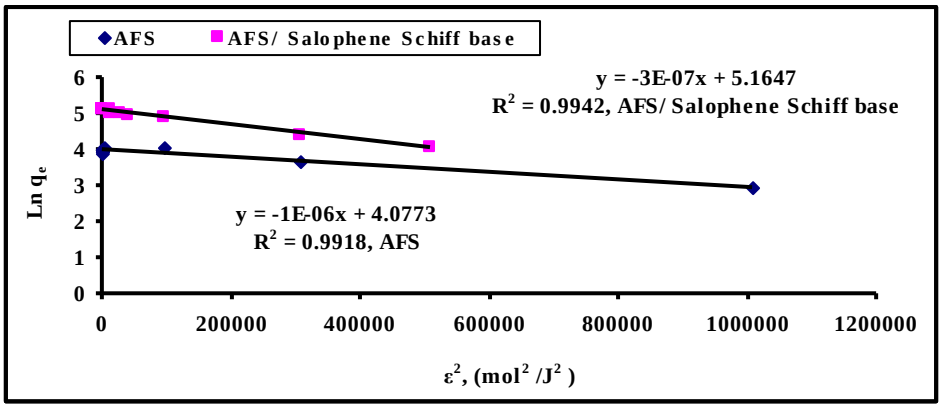

Fig. (12): Dubinin–Radushkevich isotherm for uranium adsorption onto (AFS) and (AFS/ Salophene Schiff base) composites.
Adsorption conditions: pH: 2, composite dose: 0.1 g, volume: 40 mL, temperature: room temp., time: 30 min.

The Jovanovic model is predicated on the assumptions contained in the Langmuir model, but in addition the possibility of some mechanical contacts between the adsorbate and adsorbent [65]. The linear form of the Jovanovic isotherm is expressed as follows [66]:

$$Lnq_e = Lnq_{\max} - K_j C_e \qquad (16)$$

where q_e is amount of adsorbate in the adsorbent at equilibrium (mg. g^{-1}), q_{max} is maximum uptake of adsorbate and K_j is Jovanovic constant. A plot of Ln q_e versus C_e, where K_j (Jovanovic constant) and q_{max} are calculated from the slope and intercept of the linear plots (Fig. 13). All parameters of Jovanovic are shown in Table (5). The correlation coefficient for the linear regression found to be (R^2= 0.9078 for AFS) and (R^2= 0.7586 for AFS/ Salophene Schiff base). K_j and q_{max} were determined from the slope and intercept and were found to be (-0.1887 and 14.79 mg/g for AFS) and (-0.0751 and 39.56 mg/g for AFS/ Salophene Schiff base) respectively. This suggests that the Jovanovic model doesn't fit to describe the present adsorption mechanism. It is indicated that the experiments data of Langmuir and Dubinin–Radushkevich are better than Jovanovic isotherm. According to the previous conclusion that, the achieved experimental data were fitting well with the Langmuir and Dubinin–Radushkevich isotherm.

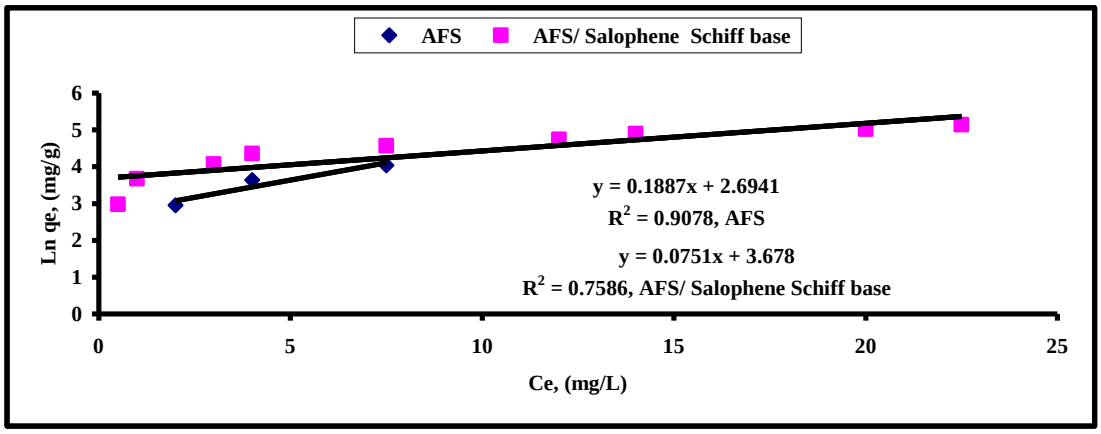

Fig. (13): Jovanovic isotherm for uranium adsorption onto (AFS) and (AFS/ Salophene Schiff base) composites. Adsorption conditions: pH: 2, composite dose: 0.1 g, volume: 40 mL, temperature: room temp., time: 30 min.

3.4. Effect of composite dose

For effective uranyl ion retention, (AFS) and (AFS/ Salophene Schiff base) dose is significant factor to be considered as it determines the sorbent-sorbate equilibrium of the system. The effect of composite dose in the range of 0.02 g to 0.2 g against uranium uptake was studied. Figure (14) reveals that the uranium uptake increases with increasing dose from 0.02 g to 0.1 g, then decreases with increasing composite dose from 0.1 g to 0.2 g for each composite of (AFS) and (AFS/ Salophene Schiff base). Therefore, the required dose to adsorb uranium ions was chosen 0.1 g. At low composite dose, all types of active sites are entirely exposed, and the surface of composite is quickly saturated. But at higher composite dose, the uranium concentration will lead to the difficulty in filling the remaining sites [67-69]. The result shows that, the maximum uptake capacities are (57 mg/g for AFS) and (171 mg/g for AFS/ Salophene Schiff base), respectively.

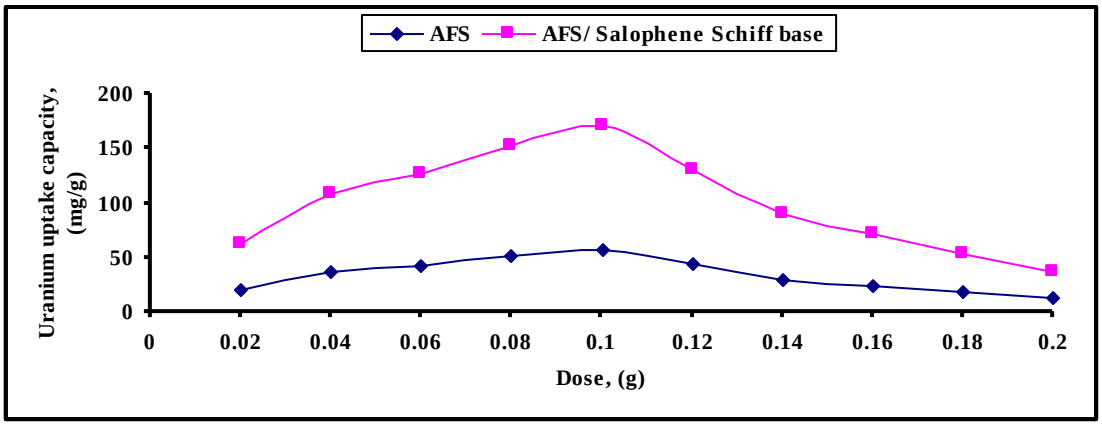

Fig. (14): Effect of (AFS) and (AFS/ Salophene Schiff base) dose on uranium uptake capacity. Adsorption conditions: Uranium conc. 150 mg/L mixed with (AFS), Uranium conc. 450 mg/L mixed with (AFS/ Salophene Schiff base), volume: 40 mL, temperature: room temp., and pH 2.

3.5. Effect of temperature

The effect of temperature on the uranium uptake is studied using 0.1 g (AFS), and (AFS/ Salophene Schiff base) contacted with 40 mL uranium solution containing conc. of (150 mg/L for AFS) and (450 mg/L for AFS/ Salophene Schiff base) at pH 2 for 30 min. at temperature from 25 ˚C to 80 ˚C. It was found that uranium uptake decreased from (57 to 24 mg/g for AFS) and (171 to 72 mg/g for AFS/ Salophene Schiff base) with increasing temperature from 25 ºC to 80 ºC. The effect of temperature as a function of uranium (VI) uptake is shown in (Fig. 15). This behavior indicates that uranium uptake onto (AFS) and (AFS/ Salophene Schiff base) is an exothermic process. Therefore, the required temperature to adsorb uranium ions was chosen at ambient room temperature. This mainly depends on the physical adsorption nature and the chelating groups in the (AFS) and (AFS/ Salophene Schiff base) matrix.

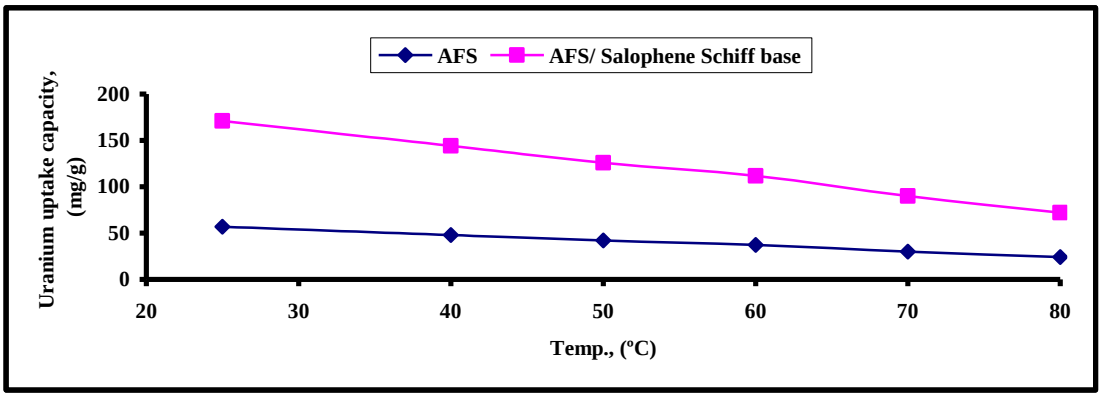

Fig. (15): Effect of temperatures on uranium uptake capacity for (AFS) and (AFS/ Salophene Schiff base). Adsorption conditions: Uranium conc. 150 mg/L mixed with (AFS), Uranium conc. 450 mg/L mixed with (AFS/ Salophene Schiff base), volume: 40 mL, composite dose: 0.1 g, and pH 2.

3.5.1.Thermodynamic studies of uranium adsorption

Thermodynamic parameters such as Gibbs free energy (ΔG°, KJ/mol), enthalpy change (ΔH°, KJ/mol) and entropy change (ΔS°, KJ/mol.K^{-1}) were studied. They were calculated from the following equations [70]:

$$\Delta G = -2.303RT\,.LogK_d \qquad (17)$$

$$\Delta G = \Delta H - T\,\Delta S \qquad (18)$$

$$LogK_d = \frac{\Delta S}{2.303R} - \frac{\Delta H}{2.303RT} \qquad (19)$$

Where R, is the universal gas constant (8.314 mol^{-1}.k^{-1}), and T, is the temperature in Kelvin (K$^{\circ}$). The values of (ΔH°, KJ/mol) and (ΔS°, KJ/mol.K^{-1}) can be calculated from the slope and intercept of the plot of Log K_d versus 1/T giving (slope of 2.4548 and intercept of -7.731 for AFS) and (slope of 2.6643 and intercept of -8.1865 for AFS/ Salophene Schiff base) respectively with a correlation coefficient, (R^2 = 0.9901 and 0.9672 for AFS and AFS/ Salophene Schiff base), (Fig.16).

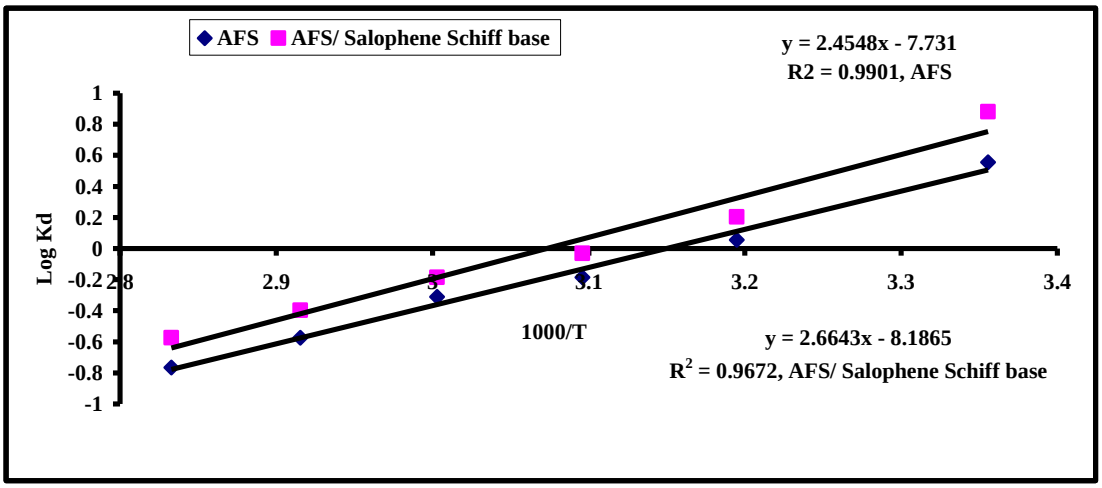

Fig. (16): Log K_d Vs 1000/T for uranium adsorption onto(AFS) and (AFS/ Salophene Schiff base). Adsorption conditions: Uranium conc. 150 mg/L mixed with (AFS), Uranium conc. 450 mg/L mixed with (AFS/ Salophene Schiff base), volume: 40 mL, composite dose: 0.1 g, and pH 2.

The results mentioned in (Table 7) indicate negative value of ΔH°, confirm that uranyl ions adsorption onto (AFS) and (AFS/ Salophene Schiff base) is an exothermic process. The negative value of ΔS°, indicate decrease in the randomness of the adsorption process in the investigated system with change in the hydration of the adsorbed uranyl ions. The negative value of ΔG°, showed that the adsorption process is spontaneous thermodynamically. Also increase in ΔG° values, from 25 $^{\circ}$C to 80 $^{\circ}$C, with increasing temperature showed that the adsorption is most unfavorable at high temperature.

Table (7): Thermodynamic parameters of uranium adsorption onto (AFS) and (AFS/ Salophene Schiff base).

Composites	ΔH°, KJ/mol	ΔS°, KJ/mol.K^{-1}	ΔG°, KJ/mol					
(AFS)	-47.00	-0.1471	298 K$^{\circ}$	313 K$^{\circ}$	323 K$^{\circ}$	333 K$^{\circ}$	343 K$^{\circ}$	353 K$^{\circ}$
			-3.174	-0.3375	+1.146	+1.981	+3.769	+5.176
(AFS/ Salophene Schiff base)	-51.01	-0.154	-5.02	-0.122	+0.185	+1.181	+2.613	+3.87

3.6. Effect of interfering ions

The tested of interference elements are chosen because these elements were composed in matrix of Abu Rusheid leach liquor. Under the adsorption optimum conditions, the effect of interfering elements were separately studied by introducing each one in 40 mL of uranium solution containing 150 and 450 mg/L mixing with 0.1 g of each composites (AFS) and (AFS/ Salophene Schiff base). The concentrations of interfering elements cause error in uranium adsorption does not exceed than ±2 %. From the obtained results shown in (Table 8), the presence of cation elements doesn't interfere with the adsorption process and could be applied for uranium extraction from cataclastic rocks, Abu Rusheid leach liquor in presence of different elements.

Table (8): The effect of interfering elements on uranium adsorption (%) onto (AFS) and (AFS/ Salophene Schiff base).

Elements	Conc., mg/L	Adsorption (%)	Elements	Conc., mg/L	Adsorption (%)
K^{+}	4000	95	Cd^{3+}	10	95
Si^{4+}	3000	95	Ba^{2+}	20	95
Al^{3+}	3000	95	Mo^{6+}	10	95
Na^{+}	2000	95	Zn^{2+}	500	94
Ca^{2+}	1000	95	V^{5+}	10	95
Mg^{2+}	1000	94	Zr^{4+}	50	94
Fe^{3+}	1500	93	Co^{2+}	10	95
P^{5+}	500	95	Cu^{2+}	20	94
Ti^{4+}	50	95	Cr^{3+}	10	95
Mn^{2+}	50	95	Pb^{2+}	20	95

Adsorption conditions: Uranium conc. 150 mg/L mixed with (AFS), Uranium conc. 450 mg/L mixed with (AFS/ Salophene Schiff base), volume: 40 mL, composite dose: 0.1 g, temperature: room temp., and pH 2.

3.7. Uranium (VI) elution and reusability procedures

Desorption is an important economic parameter in studying adsorption processes [**71**]. Three mineral acids; (H_2SO_4, HCl and HNO_3) with different concentrations from 0.1 to 1M were tested at room temperatures. A solution of 40 mL of eluting agents was allowed to elute uranium from 0.1 g of loaded composites for 30 min. From (Table 9), uranium reached to 97 % of elution efficiency with 40 mL of 0.25M H_2SO_4 from 0.1 g loaded (AFS) and (AFS/ Salophene Schiff base).

Table (9): Effect of eluting agents conc. on uranium elution efficiency from loaded (AFS) and (AFS/ Salophene Schiff base).

Concentration, (M)	Elution efficiency, %		
	H_2SO_4	HCl	HNO_3
0.10	78	60	76
0.25	97	70	84
0.50	97	81	94
0.75	97	82	94
1.00	97	85	94

Elution conditions: Volume: 40 mL, composite dose: 0.1 g, temperature: room temp., time: 30 min. and pH 2.

On the other hand, to determine the reusability of the studied (AFS) and (AFS/ Salophene Schiff base), adsorption–desorption cycles were achieved upon the composite dose using a fresh solution for each cycle under the optimum conditions. From the first to the 7th cycles, it is found that an almost complete uranium adsorption and desorption has been realized. The adsorption efficiency of the (AFS)

and (AFS/ Salophene Schiff base) were decreased from 95 to 90% in the 7th cycle. However, the desorption efficiency is decreased from 97 to 88% in 7th cycle. Therefore, it would be possible to reuse the working (AFS) and (AFS/ Salophene Schiff base) for about 7th cycles without any noticeable loss of the adsorption capacity indicating high mechanical stability in a manner to be recycled for 7th cycles.

3.8. Characterization of AFS and AFS/ Salophene Schiff base

3.8.1. ***Fourier transform infrared spectrometer characterization.***

FTIR spectra are useful tool to identify molecular functional groups [72] using FTIR model Thermo Scientific Nicolet IS10 instrument via the KBr pressed disc method in a range 400 - 4000 cm^{-1}. The FTIR spectra of each composite (AFS and AFS/ Salophene Schiff base) before and after adsorption of uranium are given in (Figs. 17 A- D).

Band at 920 cm^{-1} is assigned to Si-O asymmetric stretching vibration. The peak at 443 cm^{-1} can be attributed to the Fe–O band vibrations [73]. Bands at 680 cm^{-1} are assigned to stretching vibrations of AlO_6 octahedral [74]. The peaks at 1350 cm^{-1} represented the stretching vibration of the Al=O bond [75], (Fig. 17 A). On the other hands, the major contributions of (AFS) groups have changed, including frequency shifted, disappeared and novel bands mostly attributed to the uranium adsorption over the synthesized composite (AFS), [76, 77] (Fig. 17 B).

The band appeared at 3428.69 cm^{-1} is attributed to OH stretching vibration of water adsorbed. The peak at 3023.30 cm^{-1} is related to C=C stretching in alkenes. The -CH_2 stretching in alkanes is obtained at 2924.26 cm^{-1}. The band appeared at 1625.32 cm^{-1} is attributed to C=N stretching of imine group of (Salophene Schiff base). The peak of 1481.40 cm^{-1} is related to -NH stretching in ring. The peak at 1350 cm^{-1} represented the stretching vibration of the (Al=O) of AFS which associated with Salophene Schiff base. While, C-O, C-N stretching bands are appeared at 1219.61 and 1123.16 cm^{-1}. Band at 920 cm^{-1} is assigned to Si-O asymmetric in (AFS). The peak at 886.18 cm^{-1} is related to C=C in alkenes, strong =CH out of plane. The band of aromatic para–disub., C-H out of plane. Aromatic mono sub. is obtained at 828.57 cm^{-1}. Band at 680 cm^{-1} are assigned to stretching vibrations of AlO_6 octahedral. (Fig. 17 C).

On the other hand, after U (VI) loading onto (AFS/ Salophene Schiff base), the peaks of C–N and C=N were reduced and shifted, which suggests the coordination of the amine and imine group of (AFS/ Salophene Schiff base) to uranium ions. The OH stretching vibration disappears in the spectra of complex and the existence of water molecules appears as a broad band [78]. The FTIR spectrum of U (VI)-loaded (AFS/ Salophene Schiff base) shows an obvious shifted in the peak position and new peaks obtained related to the stretching frequency of symmetric and asymmetric dioxo uranium ion O=U=O, [79, 80]. The bands at 600 and at 750 cm^{-1} correspond to the U–O and U–N, respectively [81, 82], (Fig. 17 D).

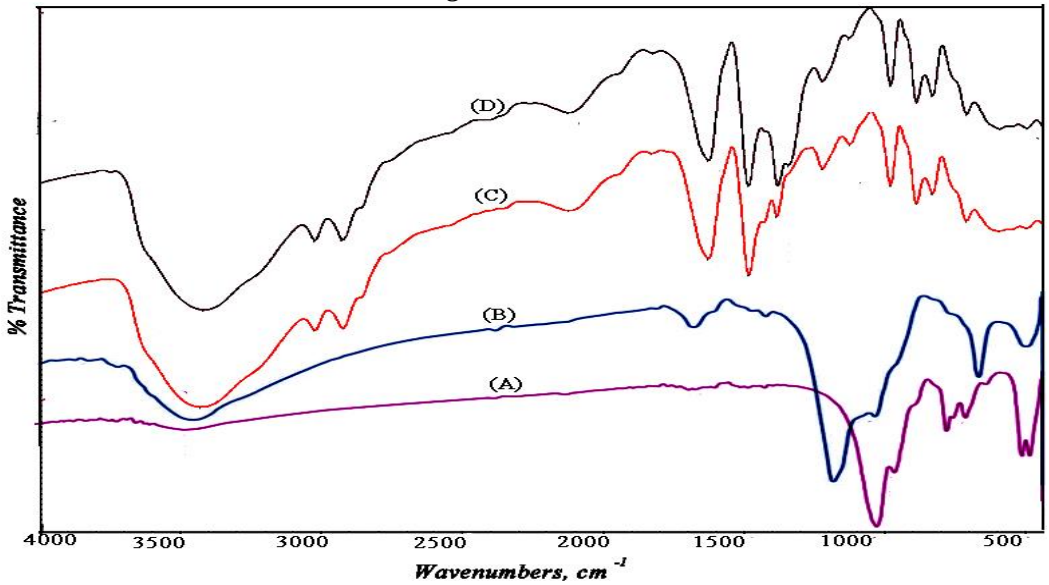

Fig. (17): FT-IR spectrum of AFS composite (A) before and (B) after uranium adsorption, AFS/ Salophene Schiff base (C) before and (D) after uranium adsorption.

3.8.2. Energy Dispersive X-Ray, (EDX) Analysis.

To identify the chemical composition of the composites before and after adsorption with uranium (VI) ions were subjected to (EDX) analysis. From (Fig. 18 A and C), the composites before loading uranium consist of (Na, Si, Fe, Al and Cl). After uranium adsorption, U (VI) ions were observed by EDX this emphasized the uptaking of uranium by (AFS) and (AFS/ Salophene Schiff base) composites as shown in (Fig. 18 B and D).

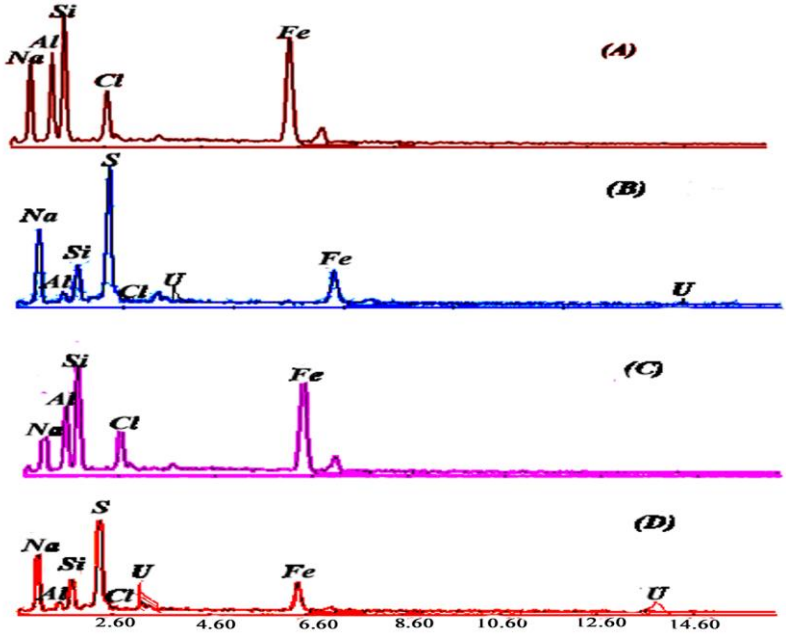

Fig. (18): EDX analysis of (AFS) composite (A) before and (B) after uranium adsorption, AFS/ Salophene Schiff base (C) before and (D) after uranium adsorption .

3.8.3. *Scanning electron microscope, (SEM)*

The SEM images of (AFS) were clearly shown the difference between the surfaces of the (AFS) before and after uranium adsorption (Figs. 19 A and B). Although a good uniformity and smooth surface was observed in the conventional composite, the surface after U (VI) adsorption was observed bright spherical spots on the composite beads. As can be seen from the results, a visible change of the surface morphology in the U (VI) adsorbed composite demonstrated that the sorption of U (VI) had taken place onto the (AFS). While (AFS/ Salophene Schiff base) composite before and after uranium adsorption were shown in (Figs. 19 C and D). After the adsorption, the pores and cracks were occupied by uranium ions.

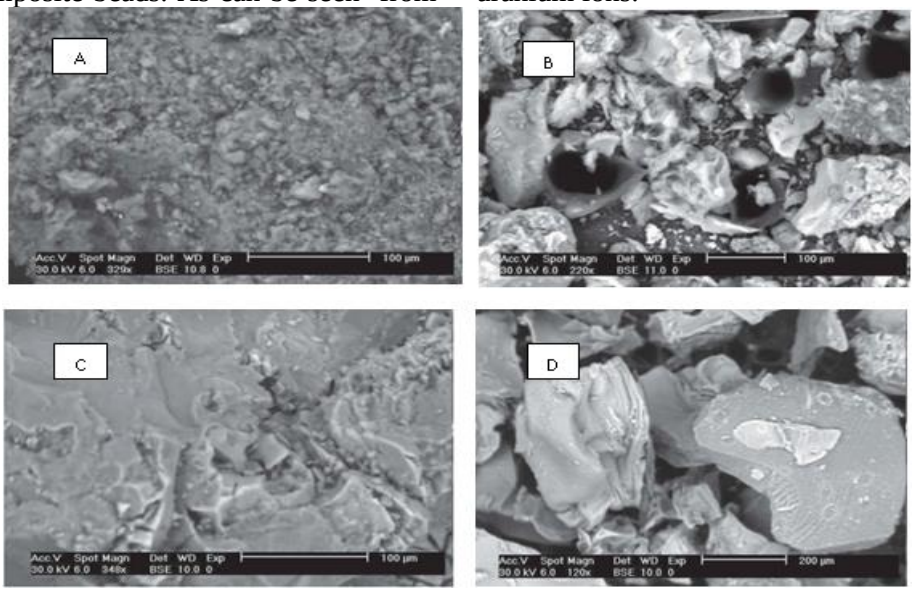

Fig. (19): SEM micrographs of AFS composite (A) before and (B) after uranium adsorption, AFS/ Salophene Schiff base (C) before and (D) after uranium adsorption .

3-8-4- Elemental analysis (CHNS)

CHNS elemental analysis of (AFS/ Salophene Schiff base) composite was obtained (Table 10).

Table (10): The CHNS elemental analysis of (AFS/ Salophene Schiff base) composite.

Composite	C	H	N	S
(AFS/ Salophene Schiff base)	60.50	16.90	9.56	4.19

3-8-5- X-ray fluorescence (XRF).

Two composites, (AFS) and (AFS/ Salophene Schiff base) after adsorption of uranium were identified by X- ray fluorescence (XRF), (Fig. 20). The XRF spectrum of composites (AFS) and (AFS/ Salophene Schiff base) show appearance of silica, aluminium, ferric, sodium, chloride and uranium. The composite of (AFS/ Salophene Schiff base) after uranium adsorption shows more affinity to uranium than (AFS), (Fig. 20).

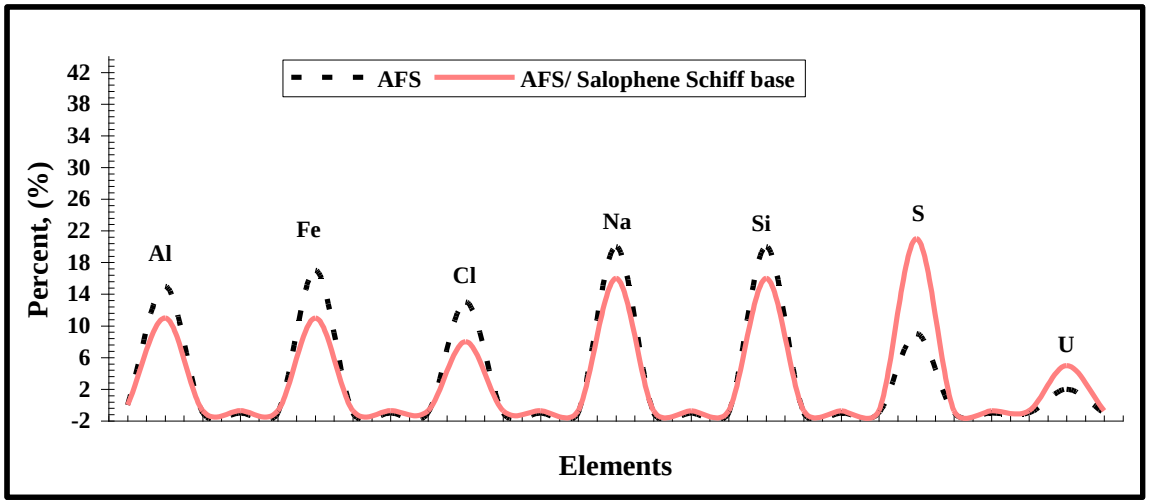

Fig. (20): XRF analysis of (AFS) and (AFS/ Salophene Schiff base) after uranium adsorption.

4-Case study

The studied technology from Abu Rusheid area with (1580 mg/Kg) uranium content was ground to -200 mesh size. This sample was subjected to acid leaching at optimum conditions: 3M H_2SO_4, 1/3 solid/liquid ratio, 200 rpm stirring speed for 2 hours at room temperature. The solution was then filtered, and uranium was measured in the leach liquor. The calculated leaching efficiency was 95 %. The obtained leach liquor has 500 mg/L for uranium. From the above data, it is evident that (AFS) and (AFS/ Salophene Schiff base) can be used to separate of uranium from sulfate leach liquor of Abu Rusheid. The applied experiments have been achieved under the previous optimum conditions by mixing 3 Liters of leach liquor assaying 450 mg/L with 2.43 g of (AFS/ Salophene Schiff base) at pH 2 for 30 min. at room temperature were achieved. In case of (AFS) composite, mixing 9 Liters of leach liquor assaying 150 mg/L with 2.28 g of (AFS) at the same previous conditions were obtained. The concentration of elements in leach liquor and effluent were subjected to analyze using ICP-OES technique to determine the content of uranium and impurities, (Table 11). Uranium was analyzed in the effluent of Abu Rusheid area about 90 mg/L which verifies that it was adsorbed with 82 %. From the obtained data, the (AFS) and (AFS/ Salophene Schiff base) composites are selective to uranium adsorption than the other metal ion impurities. On the other hand, the loaded uranium has eluted using 100 ml of 0.25M sulfuric acid. The eluted uranium was precipitated using hydrogen peroxide at pH 2 and uranium is precipitated as ($UO_4.2H_2O$). The uranium concentrate produced has uranium assay of 62% attaining a purity of 88%. To determine the uranium content and the associated metal ions, the uranium concentrate is subjected to a complete characterized using ICP-OES and XRF analysis techniques (Table 12) and (Fig.21). A comparative study for uptake capacity (mg/g) of different composites towards uranium is shown in (Table 13).

Table (11): ICP-OES specification of Abu Rusheid leach liquor and effluent (g/L).

Element	Leach liquor, (g/L)	Effluent, (g/L)	Adsorption efficiency, (%)
U	0.500	0.09	82.0
Si^{4+}	2.17	2.15	0.92
Al^{3+}	3.25	3.10	4.61
Fe^{3+}	1.22	1.20	1.63
Ca^{2+}	0.714	0.700	1.96
Mg^{2+}	0.789	0.789	0.00
P^{5+}	0.488	0.470	3.68
Na^{+}	1.96	1.95	0.51
K^{+}	3.38	3.37	0.29
Ti^{4+}	0.023	0.022	4.34
Mn^{2+}	0.036	0.036	0.00
Mo^{6+}	0.0005	0.0005	0.00
Ba^{2+}	0.016	0.016	0.00
Zr^{4+}	0.053	0.053	0.00
Cr^{3+}	0.0026	0.0026	0.00
Pb^{2+}	0.016	0.016	0.00
Cd^{3+}	0.001	0.001	0.00
Co^{2+}	0.0006	0.0006	0.00
Cu^{2+}	0.017	0.017	0.00
V^{5+}	0.0005	0.0005	0.00
Zn^{2+}	0.480	0.480	0.00

Table (12): ICP-OES specification of the prepared $UO_4.2H_2O$ from Abu Rusheid uranium concentrate.

Element	U	Si	Al	Fe	Ca	Mg	Co	Ba	Cu
Content, (%)	62.0	0.003	0.0010	0.0020	0.0100	0.0130	0.0007	0.002	0.0010
Element	Cd	Cr	Na	K	Mn	V	Zn	Pb	Zr
Content, (%)	0.0006	0.0003	0.0010	0.0100	0.0005	0.0010	0.0012	0.0013	0.0006

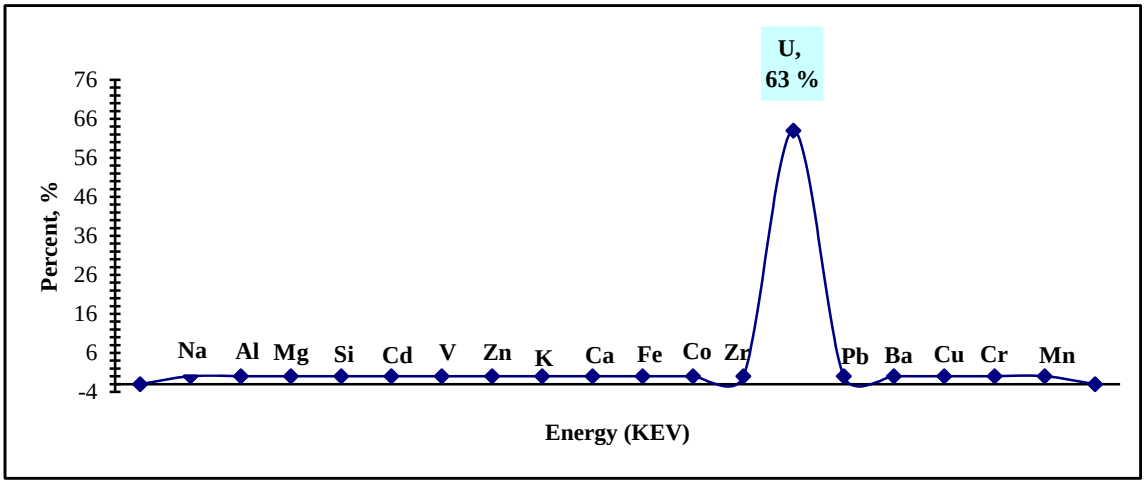

Fig. (21): XRF of the prepared $UO_4.2H_2O$ from Abu Rusheid uranium concentrate.

Table (13): The comparison of uranium adsorption capacity by different adsorbents.

Adsorbent	Q_{max} mg/g	Ref.
Rice Husk Ash with aluminium oxide composite	85	[18]
Activated carbon - Aluminium ferrisilicate (AFS) composite	142.5	[23]
Silicate mercapto Duolite composite (SMDC) composite	208.33	[24]
Manganese oxide coated zeolite modified with trioctyl amine (MOCZ/TOA)	99	[25]
Zirconium molybdophosphate composite	192.3	[26]
Bentonite treated with 1-amino 2-naphthol 4-sulfonic acid (ANSA)	90.9	[27]
Dowex50WX8 / Alizarin Red S (ARS)	121.95	[28]
Quinoline Silicate Lewatit Composite	217.39	[29]
Magnetic Schiff base (ferroferric oxide/ N,N-bis(3-methoxylsalicylidene)-1,2-phenylenediamine) composite	94.30	[32]
Aluminium ferrisilicate (AFS) composite	62.51	Present work
AFS/ Salophene Schiff base composite	175.43	

4. Conclusion

AFS and AFS/ Salophene Schiff base were used for uranium (VI) separation and adsorption from Abu Rusheid sulfate leach liquor. The obtained optimized conditions for AFS and AFS/ Salophene Schiff base at pH 2 for 30 min. at room temperature, were achieved. Under these conditions, the realized maximum uptake capacities for each (AFS) and (AFS/ Salophene Schiff base) composites have attained 62.51 mg/g and 175.43 mg/g, respectively. On the other hand, the studied thermodynamic parameters have been resulted indicating an exothermic, decreased randomness and spontaneous uranium adsorption. Also, the obtained kinetic data were found to fit pseudo-second order kinetic model. Langmuir and Dubinin–Radushkevich isotherm models are more suitable for adsorption process. Uranium can be easily eluted using 0.25M H_2SO_4 solution. The eluted uranium was precipitated as ($UO_4.2H_2O$). The uranium content in the uranium concentrate produced is 62% attaining a purity of 88%.

References

[1] M. Karve, R.V. Rajgor (2008). Amberlite XAD-2 impregnated organophosphinic acid extractant for separation of uranium (VI) from rare earth elements. Desalination, 232: 191–197. https://doi.org/10.1016/j.desal.2007.12.016

[2] A. Kilislioglu, B. Bilgin (2003). Thermodynamic and kinetic investigations of uranium adsorption on amberlite IR-118H resin. Appl. Radiat. Isotopes, 58: 155–160. https://doi.org/10.1016/S0969-8043(02)00316-0

[3] A. Rahmati, A. Ghaemi, M. Samadfam (2012). Kinetic and thermodynamic studies of uranium (VI) adsorption using Amberlite IRA-910 resin. Ann. Nucl. Energy, 39:42–48. https://doi.org/10.1016/j.anucene.2011.09.006

[4] A. Mellah, S. Chegrouche, M. Barkat (2007). The precipitation of ammonium uranyl carbonate (AUC): thermodynamic and kinetic investigations. Hydrometallurgy, 85: 163–171. https://doi.org/10.1016/j.hydromet.2006.08.011

[5] E. Herrero, M. A. Rodrigo (2020). New Electrochemical Processes for Energy and the environment (ITM/T 2019): Foreword. Electrochimica Acta, 354 (10): 136687. https://doi.org/10.1016/j.electacta.2020.136687.

[6] H. Singh, S.L. Mishra, R. Vijayalakshmi (2004). Uranium recovery from phosphoric acid by solvent extraction using a synergistic mixture of di-nonyl phenyl phosphoric acid and tri-n-butyl phosphate. Hydrometallurgy, 73: 63–70. https://doi.org/10.1016/j.hydromet.2003.08.006

[7] T.R. Prasadaao, P. Metilda, J.M. Gladis (2006). Preconcentration techniques for uranium (VI) and thorium(IV) prior to analytical determination—an overview. Talanta, 68: 1047–1064. https://doi.org/10.1016/j.talanta.2005.07.021

[8] O. Koji, S. Akhmad, T. Toshio, O. Mitsuko, M. Shoji (2009). Adsorption behavior of uranium (VI) and other ionic species on cross-linked chitosan

resins modified with chelating moieties. Talanta, 79: 1031–1035.
https://doi.org/10.1016/j.talanta.2009.03.035
[9] L.D. Pabloa, M.L. Chávez, M. Abatal (2011). Adsorption of heavy metals in acid to alkaline environments by montmorillonite and Ca-montmorillonite. Chem. Eng., 171: 1276–1286.
https://doi.org/10.1016/j.cej.2011.05.055
[10] C.J. Chisholm-Brause, J.M. Berg, R.A. Matzner, D.E. Morris (2001). Uranium (VI) sorption complexes on montmorillonite as a function of solution chemistry. J. Colloid Interface Sci., 233: 38–49.
DOI: 10.1006/jcis.2000.7227
[11] T.E. Payne, J.A. Davis, G.R. Lumpkin, R. Chisari, T.D. Waite (2004). Surface complexation model of uranyl sorption on Georgia kaolinite. Appl. Clay Sci., 26 : 151–162.
https://doi.org/10.1016/j.clay.2003.08.013
[12] M. Rafatullah, O. Sulaiman, R. Hashim, A. Ahmad (2010). Adsorption of methylene blue on low-cost adsorbents: a review. Hazard. Mater., 177:70–80.
https://doi.org/10.1016/j.jhazmat.2009.12.047
[13] A. Bhatnagar, E. Kumar, M. Sillanp (2011). Fluoride removal from water by adsorption—a review. Chem. Eng.,171: 811–840.
https://doi.org/10.1016/j.cej.2011.05.028
[14] S. Chattopadhyay, S.S. Das (2009). A simple and rapid technique for radiochemical separation of iodine radionuclides from irradiated tellurium using an activated charcoal column. Appl. Radiat. Isotopes,67:1748–1750.
https://doi.org/10.1016/j.apradiso.2009.03.114
[15] A.F. Arruda, A.D. Campiglia, B.P.S. Chauhan, P. Boudjouk (1999). New organosilicon polymer for the extraction and luminescence analysis of uranyl in environmental samples. Anal. Chim. Acta., 396 263–272.
https://doi.org/10.1016/S0003-2670(99)00448-1
[16] D. James, G. Venkateswaran, T.P. Rao (2009). Removal of uranium from mining industry feed simulant solutions using trapped amidoxime functionality within a mesoporous imprinted polymer material. Micropor. Mesopor. Mater., 119: 165–170.
https://doi.org/10.1016/j.micromeso.2008.10.011
[17] D.M. Sherm, C.L. Peacock, C.G. Hubbar (2008). Surface complexation of uranium (VI) on goethite (a-FeOOH). Geochim. Cosmochim. Acta, 72:298–310.
https://doi.org/10.1016/j.gca.2007.10.023
[18] W.M. Youssef, M.S. Hagag and A.H. Ali (2018). Synthesis, characterization and application of composite derived from rice husk ash with aluminium oxide for sorption of uranium. J. Adsorpt. Sci. Technol., 36 (5-6): 1274-1293 doi:10.1177/02636174118768920.
[19] M. Afsari, J. Safdari, J. Towfighi and M.H. Mallah (2012). The adsorption characteristics of uranium hexafluoride onto activated carbon in vacuum conditions. J. Annal. Nucl. Energy, 46: 144-151.doi:10.1016/j.anucene.2012.03.031.
[20] S.M. Yakout, S.S. Metwally and T. El- Zakla (2013). Uranium sorption onto activated carbon prepared from rice straw: Competition with humic acids. J. Appl. Surf. Sci., 280: 745-750.
doi:10.1016/ japsusc.2013.05.055.
[21] E.R. Sylwester, E.A. Hudson and P.G. Allen (2000). The structure of uranium (VI) sorption complexes on silica, alumina, and montmorillonite. J. Geochim. Cosmochim. Acta, 64: 2431-2438.
doi:10.1016/S0016-7037(00)00376-8.
[22] X. Shuibo, Z. Chun, Z. Xinghuo, Y. Jing, Z. Xiaojian and W. Jingsong (2009). Removal of uranium (VI) from aqueous solution by adsorption of hematite. J. Environ. Radioacti., 100: 162-166. doi:10.1016/j.jenvrad.2008.09.008.
[23] S.M. A. Esmaeel (2020). Sorption of uranium after carbonate leaching by low cost activated carbon–aluminum ferrisilicate composite. International Journal of Environmental Analytical Chemistry.
https://doi.org/10.1080/03067319.2020.1758685
[24] L. A. Yousef (2020). Recovery of Uranium (VI) from Sulfate Leach Liquor using Modified Duolite. Z. Anorg. Allg. Chem., 646: 340–353.
DOI: 10.1002/zaac.202000059
[25] L. A. Yousef, A. R. Bakry, A. A. Ahmad (2020). Uranium (VI) recovery from acidic leach liquor using manganese oxide coated zeolite (MOCZ) modified with amine. Journal of Radioanalytical and Nuclear Chemistry, 324:409–421. https://doi.org/10.1007/s10967-020-07042-7
[26] L. A. Yousef , A. R. Bakry , M. O. Abd El-Magied (2020). Uranium (VI) recovery from its leach liquor using zirconium molybdophosphate composite: kinetic, equilibrium and thermodynamic studies. Journal of Radioanalytical and Nuclear Chemistry, 323:549–556.
https://doi.org/10.1007/s10967-019-06871-5
[27] L. A. Yousef , A. R. Bakry , A. A. Ahmad (2020). Uranium (VI) adsorption using a mixture of 1-amino 2-naphthol 4-sulfonic acid and bentonite: kinetic and equilibrium studies. Journal of Radiochemistry, 62(4): 511-523.
DOI: 10.1134/S1066362220040086.
[28] L. A. Yousef, A. A. Ahmad and A. R. Bakry (2020). Separation of uranium ions from acetate medium by Dowex50WX8/Alizarin Red-S and its

application on granitic samples, South Um Tawat Eastern Desert. International Journal of Environmental Analytical Chemistry. https://doi.org/10.1080/03067319.2020.1772771.

[29] A. A. Ahmad (2020). Kinetics of uranium adsorption from sulfate medium by a commercial anion exchanger modified with quinoline and silicate. Journal of Radioanalytical and Nuclear Chemistry, 324:1387–1403, https:// doi.org/10.1007/s10967-020-07169-7

[30] L.T. Suručić, G.V. Janjić, A. A. Rakić, A. B. Nastasović, A. R. Popović, M.K. Milčić and A.E. Onjia (2019). Theoretical modeling of sorption of metal ions on amino-functionalized macroporous copolymer in aqueous solution. Journal of Molecular Modeling, 25, 177-189. https://doi.org/10.1007/s00894-019-4053-0

[31] M. Monier (2012). Adsorption of Hg^{2+}, Cu^{2+} and Zn^{2+} ions from aqueous solution using formaldehyde cross-linked modified chitosan–thioglyceraldehyde Schiff's base. Int. J. Biol. Macromol., 50 : 773–781.

[32] X. Zhang, C. Jiao, J. Wang, Qi Liu, R. Li, P. Yang, M. Zhang (2012). Removal of uranium (VI) from aqueous solutions by magnetic Schiff base: Kinetic and thermodynamic investigation. Chemical Engineering Journal, 198: 412–419. http://dx.doi.org/10.1016/j.cej.2012.05.090

[33] A. H. Orabi (2019). Extraction of uranium from carbonate solution using synthesized Schiff base and its application for spectrophotometric determination. Chemical Papers, 73: 1713-1730. https://doi.org/10.1007/s11696-019-00724-x

[34] L. Dolatyari, M. Yaftian, S. Rostamnia (2016). Removal of uranium (VI) ions from aqueous solutions using Schiff base functionalized SBA-15 mesoporous silica materials. J Environ Manag., 169:8–17. DOI: 10.1016/j.jenvman.2015.12.005

[35] C. Panda, V. Chakravortty, K. Dash (1987). A quadridentate Schiff base as an extractant for thorium/IV/, uranium/VI/and zirconium/IV/. J Radioanal Nucl Chem., 108(2): 65–75. https://doi.org/10.1007/BF02164692

[36] S. Sahu, V. Chakravortty (1998). Extraction of uranium (VI) with binary mixtures of a quadridentate Schiff base and various neutral donors. J Radioanal Nucl Chem., 227(1–2):163–165.https://doi.org/10.1007/BF02386452

[37] S. Sebastian, P. Singare, R. Lokhande (2013). Solvent extraction and spectrophotometric determination of Uranium (VI) using 2,2′-[1,2-phenylenebis(nitrilomethylidene)]bisphenol (BSOPD) as an analytical reagent. Int Lett Chem Phys Astron., 12:125–133. https://doi.org/10.18052/www.scipress.com/ILCPA.12.125

[38] U. Chukwu, J. Godwin (2013). Solvent extraction studies of uranium (VI) from queous media into chloroform solution of N,N′-ethylenebis(4-propionyl-2,4-dihydro-5-methyl-2-phenyl-3H-pyrazol-3-oneimine). Am Chem Sci., 3(4):479–488. DOI: 10.9734/ACSJ/2013/4155

[39] S. Verma, S. Garg, P. Kadyan (2014). Spectrophotometric determination of uranium using tris-[2,4,6-(2-hydroxy-4-sulpho-1-naphthyl azo)]-striazine, trisodium salt (THT). Chem Sci Trans, 3(1):61–66. DOI:10.7598/cst2014.587

[40] A. Bauer, A. J-schke, S. Schçne, R. Barthen, J. M-rz, K. Schmeide, M. Patzschke, B. Kersting, K. Fahmy, J. Oertel, V. Brendler, T. Stumpf (2018). Uranium (VI) complexes with a Calix [4] arene-based 8-hydroxyquinoline ligand: thermodynamic and structural characterization based on calorimetry, spectroscopy, and liquid–liquid extraction. Chem Open, 7:467–474. https://doi.org/10.1002/open.201800085

[41] K. Mathew, B. Mason, M. Morales, U. Narayann (2009). Uranium assay determination using Davies and Gray titration: An overview and implementation of GUM uncertainty evaluation. Journal of Radioanalytical and Nuclear Chemistry, 282: 939-944. doi:10.1007/s10967-009-0186-4

[42] L. Shapiro, W.W. Brannock (1962). Rapid analysis of silicates, carbonates and phosphate rocks. U.S Geological Survey Bulletin, Vol. 114 A (Revised Edition). Washington: United States Government Printing Office. DOI: 10.3133/b1144A.

[43] K. Govindaraju, C. Mevelle, C. Chouard (1976). Automated optical emission spectro-chemical bulk analysis of silicate rocks with microwave plasma excitation. Anal. Chem., 48:1325-1331. https://doi.org/10.1021/ac50003a018

[44] Z. Marczenko, M. Balcerzak, (2000). Chapter 1 - Separation and preconcentration of elements. Analytical Spectroscopy Library, 10: 5-25, https://doi.org/10.1016/S0926-4345(00)80065-6

[45] W. Davies, W. Gray (1964). A rapid and specific titrimetric method for the precise determination of uranium using iron (II) sulphate as a reductant. Talanta, 11 (8): 1203-1211. https://doi.org/10.1016/0039-9140(64)80171-5

[46] M.F. Cheira, B.M. Atia, M.N. Kouraim (2017). Uranium (VI) recovery from acidic leach liquor by Ambersep 920U SO4 resin: Kinetic, equilibrium and thermodynamic studies. Journal of Radiation Research and Applied Sciences, 10: 307-319. https://doi.org/10.1016/j.jrras.2017.07.005.

[47] M.F. Cheira, A.S. Orabi, B.M. Atia, S.M. Hassan (2018). Solvent Extraction and Separation of Thorium (IV) from Chloride Media by a Schiff Base. J. Solution Chem., 47: 611-633. https://doi.org/10.1007/s10953-018-0740-1.

[48] G. Blanchard, M. Maunaye, G. Martin (1984). Removal of heavy metals from waters by means of natural zeolites. Water Rsources, 18: 1501-1507. doi.org/10.1016/0043-1354(84)90124-6

[49] W.J. Weber, J.C. Morris (1963). Kinetics of adsorption on carbon solution. J. Sanit. Eng. Div. A. Soc. Civil Eng., 89: 31-60.

[50] R. Ahmad, R. Kumar. (2011). Adsorption of Amaranth dye onto alumina reinforced polystyrene. Clean – Soil Air Water, 39(1): 74 – 82. https://doi.org/10.1002/clen.201000125

[51] G. Crini, H.N. Peindy, F. Gimbert, C. Robert. (2007). Removal of C.I. basic green 4 (malachite green) from aqueous solutions by adsorption using cyclodextrin-based adsorbent: Kinetic and equilibrium studies. Separation and Purification Technology, 53 (1): 97 – 110. doi: 10.1016/ j.seppur.2006.06.018

[52] S.S. Gupta, K.G. Bhattacharyya (2011). Kinetics of adsorption of metal ions on inorganic materials: A review. Advances in Colloid and Interface Science, 162 (1-2): 39 – 58. doi: 10.1016 /j.cis.2010.12.004

[53] M.SA. Hagag, (2019). Comparative study of fabricated composites based on phosphogypsum and Al-hydroxide for uranium separation from aqueous and waste solutions. https://doi. org/10.1080/03067319.2019.1670826.

[54] G.E. Boyd, A.W. Adamson, L.S. Myers (1947). The exchange adsorption of ions from aqueous solutions by organic zeolites II kinetics. J. Am. Chem. Soc. 69: 2836–2848. doi.org/10.1021/ ja01203a066

[55] A.A. Siyal, M.R. Shamsuddin, M.I. Khan, N.K. Rabat, M. Zulfiqar, Z. Man, J. Siame, K.A. Azizli (2018). A review on geopolymers as emerging materials for the adsorption of heavy metals and dyes. Journal of Environmental Management, 224: 327-339. doi: 10.1016/j. jenvman.2018.07.046

[56] S.H. Chien , W.R. Clayton (1980). Application of Elovich equation to the kinetics of phosphate release and sorption on soils. Soil Sci. Soc. Am. J. 44 (2): 265-268. https://doi.org/10.2136/sssaj1980.03615995004400020013x

[57] I. Langmuir (1918). The adsorption of gases on plane surfaces of glass, mica and platinum. American Chemical Society, 40: 1361-1368. https://doi.org/10.1021/ja02242a004

[58] H. Freundlich (1906). Adsorption in solution. Physical and Chemical Society, 40: 1361-1368. https://doi.org/10.1515/zpch-1907-5723

[59] D. Ringot, B. Lerzy, K. Chaplain, J.-P. Bonhoure, E. Auclair, Y. Larondelle (2007). In vitro biosorption of ochratoxin A on the yeast industry by-products: comparison of isotherm models. Bioresour Technol, 98 (9): 1812–1821. doi: 10.1016/j.biortech.2006.06.015.

[60] H. Shahbeig, N. Bagheri, S. A. Ghorbanian, A. Hallajisani, S. Poorkarimi (2013). A new adsorption isotherm model of aqueous solutions on granular activated carbon. World Journal of Modelling and Simulation, 9 (4):243–254. ISSN 1746-7233, England, UK.

[61] K. Vijayaraghavan, T. V. N. Padmesh, K. Palanivelu, M. Velan (2006). Biosorption of nickel (II) ions onto Sargassum wightii: application of two-parameter and three-parameter isotherm models. Journal of Hazardous Materials, 133(1–3): 304–308. doi: 10.1016/j.jhazmat.2005.10.016

[62] M. R. Samarghandi, M. Hadi, S. Moayedi, F. B. Askari (2009). Two-parameter isotherms of methyl orange sorption by pinecone derived activated carbon. Iranian Journal of Environmental Health Science and Engineering, 6 (4): 285– 294.

[63] A. Dabrowski (2001). Adsorption – From theory to practice. Advances in Colloid and Interface Science 93 (1-3): 135–224. https://doi.org/10.1016/S0001-8686(00)00082-8

[64] M.M. Dubinin (1960). The potential theory of adsorption of gases and vapors for adsorbents with energetically non-uniform surface. Chemical Reviews, 60 (2): 235–241. https://doi.org/10.1021/cr60204a006

[65] S. K. Knaebel (2004). Adsorbent selection. International Journal of Trend in Research and Development, Adsorption Research, Incorporated Dublin, Ohio. 43016.

[66] A. V. C. Kiseler (1958). Vapour adsorption in the formation of adsorbate Mollecule Complexes on the surface. Kolloid Zhur, 20: 338–348.

[67] D.P. Das, J. Das, K. Parida (2003). Physicochemical characterization and adsorption behavior of calcined Zn/Al hydrotalcite-like compound (HTlc) towards removal of fluoride from aqueous solution. Colloid Interface Science, 261: 213 - 220. doi:10.1016/S0021-9797(03) 00082-1

[68] X.P. Liao, B. Shi (2005). Adsorption of fluoride on zirconium (IV)-impregnated collagen fiber. Environ. Sci. Technology, 39: 4628 - 4632. doi**:** 10.1021/es0479944.

[69] N. Chaudhary, C. Balomajumder (2014). Optimization study of adsorption parameters for removal of phenol on aluminum impregnated fly ash using response surface methodology. Taiwan Inst. Chem. Engineering, 45: 852–859. doi:10.1016/j.jtice.2013.08.016

[70] B.M. Atia, M.A. Gado, M.O. Abd El-Magied, E.A. Elshehy (2019). Highly efficient extraction of uranyl ions from aqueous solutions using multi-chelators functionalized graphene oxide. Separation Science and Technology, 1-12. https://doi.org/10.1080/01496395.2019.1650769.

[71] B. Kannamba, K.L. Reddy, B.V. Apparao (2010). Removal of Cu (II) from aqueous solutions using chemically modified chitosan. Hazardous Materials, 175: 935–948. doi:10.1016/j.jhazmat.2009.10.098

[72] J. Dong, Y. Ozaki (1997). FTIR and FT-Raman studies of partially miscible poly (methy1 methacrylate) /poly(4-vinylphenol) blends in solid states. Macromolecules, 30: 286-292. doi: 10.1021/ma9607168

[73] A. Lassoued, B. Dkhil, A. Gadri, S. Ammar (2017). Control of the shape and size of iron oxide (α-Fe_2O_3) nanoparticles synthesized through the chemical precipitation method. J. Res. In Phys., 7: 3007-3015. doi:10.1016/j. rinp.2017.07.066.

[74] D.C.L. Vasconcelos, E.H.M. Nunes, W. L. Vasconcelos (2012). AES and FTIR characterization of sol–gel alumina films, Journal of Non-Crystalline Solids 358(11):1374–1379. DOI: 10.1016/j.jnoncrysol.2012.03.017

[75] S. Lagergren (1898). Zur Theorie der Sogenannten Adsorption Gelöster Stoffe. Bihang till Kungliga Svenska Vetenskapsakademiens, Handlingar 24 (4) :1–39. https://weburn.kb.se/metadata/824/EOD_2758824.htm.

[76] E. Guibal, C. Roulph, P. Cloirec (1995). Infrared Spectroscopic Study of Uranyl Biosorption by Fungal Biomass and Materials of Biological Origin. J. Environ. Sci. Technol., 29: 2496-2503. doi:10.1021/es00010a007.

[77] G. Blázquez, M.A. Martín-Lara, G. Tenorio, M. Calero (2011). Batch biosorption of lead (II) from aqueous solutions by olive tree pruning waste: Equilibrium, kinetics and thermodynamic study. J. Chem. Eng., 168: 170-177. doi:10.1016/j.cej.2010.12.059.

[78] A. H. Orabi, S. A. Elenein, Sh. S. Abdulmoteleb (2019). Amberlite XAD-2010 Impregnated with Chrome Azurol S for Separation and Spectrophotometric Determination of Uranium and Thorium. Chemistry Africa, 2: 673–688. https://doi.org/10.1007/s42250-019-00072-z

[79] A. El-Sonbati, M. Diab, A. A. El-asmy (1989). Uranium (VI) complexes of some schiff bases derived from hydroxyaromatic aldehyde and ketone. Synth React Inorg Met Org Chem, 19(7):731–740. https://doi.org/10.1080/00945718908048107

[80] I. Yilmaz, H. Temel, H. Alp (2008). Synthesis, electrochemistry and in situ spectroelectro-chemistry of a new Co(III) thio Schiff-base complex with N,N′-bis(2-amino thiophenol)-1,4-bis(carboxylidene phenoxy) butane. Polyhedron, 27 (1):125–132. https://doi.org/10.1016/j.poly.2007.08.044

[81] M. Salam, S. Jahangir, D. Chowdhury, Z. Siddique (1997). Dioxouranium (VI) complexes of some dibasic tridentate ONO donor ligand systems. Chittagong Univ Stud Part II, 21(1):23–28.

[82] D. Chowdhury, M. Uddin, M. Sarker (2008). Synthesis and characterization of dioxo uranium(VI) complexes of some aroylhydrazines and their Schiff bases with acetone. Chiang Mai J Sci., 35(3):483–494.